

Approval Sheet

Title of Thesis: Hierarchical, Low-Cost Person Detection System for Rescue and Relief

Name of Candidate: Babur Nawaz Khan
MS Computer Science, 2015

Thesis Approved By: _____
Dr. Charles Nicholas
Professor
Department of Computer Science and
Electrical Engineering

Date of Approval: _____

Abstract

Title of Thesis:

Hierarchical, Low-Cost Person Detection System for Rescue and Relief

Babur Nawaz Khan, MS Computer Science, 2015.

Thesis Directed by:

Dr. Charles Nicholas, Professor

Department of Computer Science and Electrical Engineering.

In recent times, intelligent, unmanned vehicles with onboard computers and sensors have been used in many ways for better serving humanity. An important use case of such vehicles is the deployment in the field of Disaster Rescue and Relief. Many remote controlled systems have been tested in real life disaster situations, with dramatic increase in productivity of Rescue and Relief teams and a huge decrease in loss of precious lives. These systems, however, are not cost effective and thus, out of reach of most organizations involved in these activities. Based on these observations, I felt that a generic and robust system which is also affordable and easily deployable/manageable is the need of the hour. These factors, along with the availability of affordable technology, motivated me to focus my research on the use of thermal imagery for person detection from Unmanned Aerial Vehicles (UAVs) in disaster situations. The person detection system works in a hierarchical, multi-phase deployment, with each step having its own significance. The onboard thermal and Raspberry Pi cameras record images at a pre-determined interval, which are processed for detection onboard the UAV's computer. These images are compressed and wirelessly sent to the ground control station, along with the UAV flight status information (location co-ordinates, airspeed, ground-speed, and altitude) at a near real-time speed. The ground control system organizes the data and is responsible for alerting users when successful detections are made. The system's use of mesh network architecture makes it highly scalable and flexible, with various multi-nodal deployment options.

Hierarchical, Low-Cost Person Detection System for Rescue and Relief

By
Babur Nawaz Khan

Thesis submitted to the Faculty of the Graduate School of the
University of Maryland Baltimore County in partial fulfillment
of the requirements for the degree of
Master of Science
2015

Advisory Committee:

Dr. Charles Nicholas / Advisor

Dr. Muhammad Younis

Dr. Ting Zhu

© Babur Nawaz Khan 2015

All Rights Reserved

Dedication

To my late father, Muhammad Nawaz Khan, whose unquenchable thirst for knowledge and education, inspired and enabled me to pursue higher education in the United States of America.

To my mother, Musarrat Nawaz, for always motivating and supporting me through thick and thin, and for always remembering me in her prayers.

To my siblings, for always being there for me. Without their guidance this journey would not have been so easy.

Acknowledgments

I would like to thank Dr. Charles Nicholas for the support and supervision he provided throughout the lifetime of this research project. Without your time and efforts, I would have been totally lost.

I would also like to thank Dr. Ting Zhu for opening the doors of his lab to me and for lending me the resources that made this research possible.

I am grateful to my colleague Amer Tahir for his support, guidance and equipment, which helped form the basis for this research.

Table of Contents

- Chapter 1 Introduction..... 1**
- 1.1 Motivation..... 4**
- 1.2 Structure of this document..... 6**
- Chapter 2 Literature Review 7**
- Chapter 3 System Design and Architecture 10**
- 3.1 Hardware Design and Architecture 10**
- 3.2 Software Design and Architecture..... 21**
- 3.3 Deployment Architecture 23**
- Chapter 4 Experimentation 26**
- 4.1 Environmental Metrics..... 26**
- 4.2 Test Plans..... 29**
- Chapter 5 Evaluation and Discussion 38**
- 5.1 Prototype A..... 39**
- 5.2 Prototype B 42**
- 5.3 Prototype C..... 46**
- Chapter 6 Conclusion 52**
- 6.1 System Limitations and Problems Encountered 53**
- 6.2 Future Work..... 55**
- Appendix 57**
- References..... 58**

List of Tables

Table 3.1 FLIR Lepton Camera Models	14
Table 3.2 Comparison of Prototypes	19
Table 4.3 Prototypes and relevant Metrics	31
Table 5. 1 Optimal Operational Recommendations	50

Table of Figures

Figure 3. 1 3dr X8+ Octo-Copter.....	11
Figure 3. 2 Raspberry Pi 2	13
Figure 3. 3 Pixhawk	13
Figure 3. 4 Raspberry Pi Camera Module.....	15
Figure 3. 5 Xbee Pro 900	15
Figure 3. 6 External, Internal Top And Bottom Views Of Ublock GPS Module	16
Figure 3. 7 Prototype B With All The Components Attached	17
Figure 3. 8 Prototype B With Flir Lepton And Pi Camera Module Installed	18
Figure 3. 9 Prototype C With The Remote Radio Controller.....	19
Figure 3. 10 Hardware Architecture (Uav)	20
Figure 3. 11 Hardware Architecture (Ground Control Station)	20
Figure 3. 12 Uav Software Architecture	21
Figure 3. 13 Three Types Of Rescue Operations	24
Figure 3. 14 Multi Unit Deployment With A Mesh Network	25
Figure 4. 1 Images Captured With Prototype A, With MSER Blob Detection.....	30
Figure 4. 2 A) Image Taken At 5 Meters B) Same Posture At 20 Meters, C) Object Viewed At 40 Meters	31
Figure 4. 3 A) Image Taken At 5 Meters B) Same Posture At 20 Meters, C) Object Viewed At 40 Meters	32
Figure 4. 4 A) Image Taken At 5 Meters Over Asphalt Path B) Same Posture At 20 Meters, C) Object Viewed At 40 Meters	32

Figure 4. 5 A) Image Taken At 20 Meters With Test Subject Moving Away From The Drone At 5 Kph B) Moving Towards The Drone At 7 Kph, C) Running Away At 15 Kph.....	33
Figure 4. 6 A) Image Taken At 20 Meters With The Drone Flying At 1 Kph B) Flying At 2 Kph, C) Flying At 4 Kph	33
Figure 4. 7 A) Image Taken At 10 Meters Simulating Floods And B) Submerged Legs Of The Test Subject Seen.....	34
Figure 4. 8 A) Subject At 7 Meters, B) Subject At 15 Meters And C) At 15 Meters With A Side Drift ..	34
Figure 4. 9 A) Subject At 7 Meters, B) At 15 Meters And C) At 15 Meters With A Side Drift	35
Figure 4. 10 Thermal Images Captured At Altitudes Of 7, 12 And 15 Meters Respectively	35
Figure 4. 11 Color Images Recorded At Altitudes Of 7, 12 And 15 Meters Respectively	36
Figure 4. 12 Images Captured At An Altitude Of 12 Meters.....	36
Figure 4. 13 MSER Stage 1 Applied To Multiple Frames From Different Tests	37
Figure 4. 14 MSER Stage 2 Applied To Stage 1 Frames. Note That The Last Frame Shows No Detection And Makes A False Negative Judgement.	37
Figure 5. 1 Performance of Prototype A based on Surface Type.....	40
Figure 5. 2 Performance of Prototype A based on tests conducted at Day time	41
Figure 5. 3 Overall Performance of Prototype A	41
Figure 5. 4 Pie Chart showing True VS False values.....	42
Figure 5. 5 Performance of Prototype B based on Surface Type at Night Time.....	43
Figure 5. 6 Performance of Prototype B based on Surface Type at Day time	44
Figure 5. 7 Comparison of Day and Night testing for Prototype B	44
Figure 5. 8 Overall performance of Prototype B.....	45
Figure 5. 9 True VS False value comparison for Prototype B	46
Figure 5. 10 Performance of Prototype C based on Surface Type.....	47
Figure 5. 11 Performance of Prototype C based on Weather conditions	47
Figure 5. 12 Performance of Prototype C based on Day Time testing.....	48
Figure 5. 13 Overall Performance of Prototype C	49
Figure 5. 14 Comparison of True and False values for Prototype C.....	49
Figure 5. 15 Comparison of overall performance numbers for all prototypes	50
Figure 6. 1 The Lepton's two models, with Zoom and FOV information.....	54

Chapter 1

Introduction

Person detection through automated systems has always been a subject of great interest within the realm of Information Technology and Engineering. Due to the vast range of uses for these systems, a lot of research has been carried out in this area. In recent years, a lot of research has been done in the area of Person detection techniques and systems and it has been a hot topic in Computer Science. Better optics, along with the availability of publically accessible, open source and flexible software makes this area even more interesting. Improvement of thermographic and infrared cameras also played an important role in the advancement of the field of person detection. These cameras and imaging techniques are commonly used in military deployments, the field of medicine, infrastructure inspections, and area mapping etc.

In the past, airborne person detection systems, especially the ones that employ the use of thermal or infrared imagery have primarily been used by the world militaries for surveillance and reconnaissance purposes, the area is gaining more importance every day and scientists and engineers have come up with new, wider use cases for these systems. UAVs with imaging systems have also been extensively used in the fields of agriculture, land surveys, aerial photography, delivering medicines and other supplies.

Since Hurricane Katrina [1] hit the coastal areas of the United States in 2005, such systems have been vastly deployed throughout the world for disaster search and rescue operations. UAVs

that were used during the war in Iraq and Afghanistan were deployed in areas of New Orleans. Since these aircrafts had thermal imaging systems, they could be used to locate survivors trapped inside the buildings.

Low cost unmanned aerial vehicles (UAVs) that are field ready at a moment's notice and easily deployable have made advancements in this direction possible. These systems are somewhat disposable, pose less of a threat to the surroundings in case of an emergency while giving the operatives an opportunity to control them from a safe distance. The fact that these UAVs are commercially available gives operators the freedom from any military restrictions that they might have had to face in the past. The introduction of new and superior thermal uncooled cameras have also allowed for the deployment of UAVs with better results.

One of the main reasons UAVs are used in disaster situations is that once a disaster hits an area, the terrain can be deemed unfit for traversal by land vehicles. For example, during the 2008 earthquake that struck the northern areas of Pakistan, people were stranded in far off villages that were hard to reach even in normal times, let alone in the aftermath of a major disaster. The result was high rates of losses, with even higher long term displacement numbers. People were not reached on time and that in turn caused for much greater problems. Another example is the case of Hurricane Katrina. Since vast areas were affected, with debris scattered over miles, Unmanned Ground Vehicles (UGVs) could not be deployed. The terrain in the aftermath of the disaster had become highly unpredictable that delayed land response as well, resulting in the loss of precious time that could have been used towards the mitigation of the situation. In the above examples, UAVs were the only machines that could be deployed safely, traversing over large areas and gathering large amounts of data while providing the rescuers with a bird's eye view of the whole situation on the ground.

Keeping the above discussion in mind, I have proposed this research project which tries to tackle different issues related to aerial person detection systems. The primary purpose of this research project is to provide a basis for a cost effective, unmanned, aerial person detection system that uses latest techniques and equipment for achieving its main goals. The system is also meant to provide a solution that is easily deployable and highly scalable, both in terms of monetary restrictions as well as technical ones. The system is developed so that it can minimize response times for rescue teams and organizations working in the field. The system is also purposed to provide maximum amount of information about a large area in the minimum possible time, which will improve response times by a huge factor.

The system presented in this research is based on a multi-tier system that aims to ease the burden off of the UAV and making for easier deployment. The system is based around the functionality of a custom designed thermal sensor that has been employed for use in this project even though it was not built for this purpose. The system also provides real color images captured by an off-the-shelf optical camera for mapping purposes and for providing the human operators with sufficient information so that environmental and situational awareness can be enhanced, providing for better planning and deployment.

The thesis is primarily focused on cost reductions in person detection using UAVs. The price reduction is achieved by taking into account multiple factors. One of the main factors that affects the low cost of the system is the choice of UAV platform. Our system is designed for smaller, more cost effective UAV platforms that can be bought ready to fly from many commercial vendors which makes the system very versatile in its deployment. Another price reduction point is the use of cost effective thermal imagery and color imagery cameras, namely the FLIR Lepton and the Raspberry Pi camera modules. These factors reduce the price of the system phenomenally and help us achieve the main objective of keeping the cost within a low budget as well as having the system capable of deployment on small sized, commercially available UAVs.

The system uses an onboard computer i.e. the Raspberry Pi 2 which is used as a primary computer for image detection. Another onboard computer, the drone's flight controller is also used to gather flight data that can provide vital information to the operators which can help in localization of victims. The Pi is also responsible for gathering the images that have had detection algorithms implemented to them, gathering flight data from the flight controller, packetizing the data collected using a custom packetization algorithm which enables the Pi to send the data using cost effective equipment, processing and buffering the data, and then transmitting the categorized data to the ground control station. At the ground control station, the data is processed as part of the second tier of the hierarchical system.

In the second phase, the data is re-organized, and presented to the user, with necessary prompts and alerts. The second phase of the system also makes use of maps that visually display the information captured during a flight mission. Use of maps enhances the understanding and learning of users and humanizes the data collected.

The system was cultivated with a prototype based development model in mind. This was more due to limitations and restrictions faced during the lifetime of this project. The first two prototypes use different thermal sensors while using the same code base and UAV. The third and final prototype was created using a modified code and a totally new UAV, with better stability and finesse.

The prototypes were each tested extensively in the outdoors with the UAVs and ground control systems in full action. Real life test subjects were used in a number of simulated scenarios which were meant to mimic real life disaster environments. Person-UAV relative movements were taken into account when gathering information during the experimentation phase of this project since simulating real life scenarios was the main objective of the experiments. At the same time, to get better results, tests were conducted with the UAV deployed in loiter mode (hovering) with stationary test subjects so that maximal exposure could be gained. Tests were also carried out at various altitudes and relative speeds so that more globalized scenarios could be simulated.

Results derived from these experiments show that the detection rates are fairly acceptable. It is also determined that the equipment used in these experiments give far better results than expected. The thermal sensor surpasses its intended usage and can be established as an essential future UAV deployable part. The system is of course limited due to the main objective of keeping

the system highly cost efficient, but outperforms many commercially available systems nonetheless.

1.1 Motivation

The disaster management process can be broken down into three stages: The Search and Rescue Phase, where the first responders are deployed with a focus on saving as many lives as possible. The second stage is the Relief Phase, where relief goods are sent to the organizations working on the ground, who in turn distribute these goods to the survivors of the disaster. The third and final stage is the Rehabilitation Phase during which the displaced people are provided with the necessities and infrastructural help that they need to repatriate back to their homes. These phases take months, usually years to complete.

In the past decade, countries like Pakistan, Japan, Indonesia, The United States, India, Bangladesh, Haiti, and Nepal have been struck by large magnitude disasters of different types e.g. earthquakes, tsunamis, floods etc. These disasters have caused billions of dollars' worth of damages in these countries, with thousands of casualties and large scale displacement of people recorded particularly in Pakistan. Most of the names listed here are of developing countries with limited resources to tackle such large scale crises. With most infrastructure destroyed or damaged by the disasters, especially earthquakes, people are stranded for days, weeks and sometimes even months and help can take many days to come to them. These countries mostly rely on foreign aid in such situations which causes further delays and precious time at the beginning of the disaster relief process is lost.

According to Dr. Robin Murphy, Director of the Center for Robot-Assisted Search and Rescue (CRASAR), around one million people die as a direct result of disasters all over the world. Death is not the only infliction caused by these disasters as over two and a half million people are left permanently disabled or displaced. The displaced communities are estimated to require anywhere from 20 to 30 years to fully recover from the damages caused by these disasters. On top of all of this, billions of economic losses also result as a by-product of these disasters, mostly due to infrastructure destruction or damages [2].

Dr. Murphy states that if initial disaster response time can be reduced by a single day, then the overall relief and recovery process can be sped up by a factor a thousand days, which is over three years. This is because a chain reaction is set within the disaster management process itself. If the first responders and rescuers can get in with accuracy and save lives as soon as the disaster strikes, it can clear the way for secondary groups to get into action. These groups include engineers and construction workers who can move in and start work on damage assessment and initial repairs to the infrastructure. The sooner repair work can be started, the better for the victims of the disaster as they can be rehabilitated sooner. Major insurance companies state that if claims are made even a single day earlier, that sets off a ripple action that can make a difference of up to six months in the person getting their home repaired.

According to the above stated facts, the best way to reduce the overall effects of a disaster is to focus on the disaster Search and Rescue (SAR) stage and to improve on the response time for the rescue teams. Taking this into account, this research was carried out, with a focus on the detection of people from a UAV in such a way that it can be used to effectively detect survivors, directing rescuers to their location with maximal accuracy so that the number of fatalities can be minimized.

The reason an Unmanned Aerial Vehicular solution was proposed is because UAVs are very handy for monitoring environmental disasters (natural and otherwise), because of their ability to traverse terrains that can be very difficult for regular humans to do. The use of thermal cameras increase visibility in difficult weather conditions after a disaster and also enhance person detection abilities of the rescuers since the thermal imagery can be used to determine if a victim is alive or not. UAVs can also prove handy in large scale mapping of affected areas, giving an overview of the situation, based on which further planning can be done.

Current robotic solutions are not cost effective and are mostly out of the reach of small organizations. These small organizations can prove to be the difference between life and death in such situations. Even government-run organizations in most countries listed above cannot afford highly expensive solutions due to budget restrictions. Therefore, this research project aims to reduce these costs and concentrates on providing an exceedingly cost effective UAV based mobile person detection system which can provide quality results at less than quarter of the price of other commercially available and military systems. For example, the high-end prototype of this project costs no more than \$2200 while the cheapest commercial robot costs a minimum of \$10,000, meaning this project costs over four times less compared to the cheapest thermal person detection system readily available. All these factors make for a highly scalable solution that can be deployed anywhere in the world.

Some advantages of Search and Rescue (SAR) operations that employ UAVs include:

- UAVs compared to other alternatives are inexpensive and somewhat disposable. Risk in data collection right after a disaster is fairly low compared to the alternatives of sending teams in with little to no information about the disaster or terrain changes after the disaster.
- UAVs provide wide angles of observations, depth, detail and flexibility that traditional means of distant observation like binoculars, airplane surveillance and satellite imagery cannot provide.
- UAVs also allow for rapid deployment and quick assessment of damage.
- UAVs can also be used for mapping movement of affected people and temporary settlements in a disaster stricken area.

1.2 Structure of this document

In this chapter we were introduced to the problem at hand and an overview of the solution that we have devised. We also had a look at the disaster management process and how our system can be placed inside that process.

The rest of this thesis document is structured as follows:

- Chapter 2 talks about the prior work in the area of person detection using UAVs and thermal imagery.
- Chapter 3 takes us into the details of the design of the solution in terms of the Hardware and Software components used. We also discuss the deployment of the system in this chapter.
- Chapter 4 describes the experimentation and test cases used for the evaluation of this system.
- Chapter 5 goes into the details of results that the system produced. A detailed discussion about these results is also part of this chapter.
- Chapter 6 gives a brief conclusion of this research and points out the problems encountered as well as the limitations of the system. This chapter also lists points for possible future work and improvements that can be made.

Chapter 2

Literature Review

This chapter sheds some light on similar research conducted in the past by other scholars. Most of the previously done work has focused on person detection using on-ground thermal imagery trying to mimic similar settings for a UAV. This chapter provides an overlook of what has previously been done in the field of UAV based detection systems and the use of thermal imagery, the methods and techniques used, the results and how all of that relates and implies to the work conducted for this research.

A detection and tracking system was proposed in by Portmann et al. that processes thermal image sequences captured from the viewpoints similar to the ones from a UAV. The tracking framework consists of a pipeline that uses background subtraction method along with a particle filter guided detector resulting in high recall rates and high precision. Even if their system uses cameras mounted on buildings, the tracking framework is meant to work if the setup experiences unsteady motion to emulate the setup on a UAV [3].

Background subtraction provides for faster detection by reducing the search space for the people detector, the most time consuming part of the process. The subtraction method used in this research only processed thermal (long-infrared) wavelengths that makes tracking possible at night and other situations where visible-light camera resolution and image quality would be limited. Four different detectors were used to test the performance at different levels. The system used different datasets to train Histograms of Oriented Gradients (HOG), which uses pre-trained model for comparing the object. LatentSVM, an extension of HOG that is not only capable of detecting the objects of exact same shape but also in different configurations, takes the position of the detected parts in account to return a value instead of classifying an object as a whole. Another detector concept that is based on Local Binary Patterns (LBP) uses a binary test to gradually filter

out non-matching objects. This technique uses a center pixel and compares its intensity with the intensity of pixels around the center pixel allowing for high detection rates. For Body Part based Detection (BPD), the training was focused on head, upper body and legs and applies a sliding window approach. Each identified particle is assigned a weight, based on how well they represent an object, used to determine future location of the object. The system requires a choice of detector along with particle filter framework and the research illustrates the difference and comparison of results by using each of the detectors. All of these processes are CPU intensive and require a computer more powerful compared to the ones we have used in this research. This can hinder mobility, therefore rendering a compact UAV based deployment of the system, invalid.

Molina et al. however, focus on the CLOSE-SEARCH project which uses a medium-sized helicopter-like drone and integrates it with thermal imagery and a multi-sensor navigation system or aerial person detection [4]. The prototype includes Unmanned Aerial Systems (UAS) system that consists of UAV and Ground Control Station (GCS). The GCS is characterized with a navigation subsystem with very high accuracy and altitude determination that is used to validate EGNOS-based navigation subsystem. Project also focuses on Beyond-Line-of-Sight communication. The prototype establishes two data links which include a downlink to transmit the data and uplink to send commands, and a downlink to transmit images and other remote sensing outcomes. The project uses WiFi as primary and WiMax as secondary technology strategies for communication. Real life SAR (Search and Rescue) crews helped with deployments of the system in realistic scenarios and trained SAR operators looked to identify a person, eliminating the use of algorithms. Thermal and RGB cameras were used for experimentation. Several requirements like endurance, safety, application performance and others were kept in mind from navigation standpoint which becomes important when analyzing and interpreting the outcome. Integrity of the system, use of UAV, navigation were given special attention resulting in more accurate outcomes. Initial testing in a lab assessed the integration of all subsystems and a real-life testing scenario was designed to demonstrate how the system would work in a real life scenario. This project is not cost effective and requires a huge capital investment, thus making it counter intuitive in terms of scalability.

Rosendall in his study, examines the effectiveness of several algorithms used to detect humans [5]. The two distinct domains used for detection in this study are leave-behind sensing and aerial surveillance. Both algorithms used in the study had a very high success result rate. The three main elements that were used to choose an algorithm for testing included the ability to implement the software so that results can be verified, demonstrated success with tough datasets, offline training and online runtime testing. These elements held significance at different levels for the study. For leave-behind sensing domain, a more realistic and independent dataset was used to train and test the HOG algorithm. As the detection system ran faster than the video used for testing, real-time person detection becomes more realistic using the algorithm with image subtraction. Around 95% of images were successfully identified in another enhanced version of a standard model of visual cortex, called HMAX, for aerial surveillance domain. The images taken from a vertical height, with human presence were cropped manually to mimic the image that isolate other foreground objects using registration techniques. The success of both domains demonstrate the potential of person detection by introducing a realistic and independent set of data for training and

then testing. Other methods used in the study include Viola and Jones' Boosted Cascade algorithm (V-J) that utilizes statistical modeling to classify images or presence of objects in the image. This algorithm has been effective in frontal face recognition with very low detection time. There are several other algorithms that were assessed for this study but were not focused on. Overall, the study demonstrated the potential of the mentioned algorithms in the field of person detection with relevant training.

Portmann's research was primarily based on non-UAV systems deployed on rooftops as well as long sticks, simulating UAV viewing angles. This does not help in our case because the system was not deployed on real UAVs or a smaller, limited computer like the Raspberry Pi. The methods they used require high CPU usage and the Pi cannot provide the same processor performance. For the Molina et al. method, a high cost, powerful, medium sized drone was required which in our case defeats the purpose of the whole research since we are trying to minimize the costs. The sensors used in that research project are also very high cost and even though they provide us with the best results, they are still not in line with our objectives. Finally, for the method utilized by Paul Rosendall, we observe that even though the success rate of person detection is phenomenally high at 95%, it is still not deployable on a small system like ours, using a Raspberry Pi. The reason for this being that the algorithms used in the study require high CPU usage and large memory resources, which are not available when using a Raspberry Pi.

Chapter 3

System Design and Architecture

This chapter discusses the details of the Hardware and Software design of the system. Design of the UAVs used over the course of the project are discussed in detail along with the components used i.e. the cameras, Raspberry Pi, antennas and others. Software design is also discussed in detail, focusing on how the software components in the UAV and Ground Control System integrate with each other.

This system also discusses the deployment design of the system. Questions like what topology is being used, what the system would look like in theory, and what areas of a disaster related deployment would the system be used in etc.

3.1 Hardware Design and Architecture

This project made use of three different prototypes for testing purposes. Prototypes were differentiated between based on the equipment used. Prototypes were named alphabetically, each prototype having changes listed in relevant areas. Each prototype saw very minor changes in terms of software design therefore those changes are discussed in section 3.2. We will look at the details of each hardware component as follows:

3.1.1 UAVs

Two different kinds of UAVs were used over the course of this research project's lifetime. The first UAV was the X8+ by 3D Robotics. It was an extremely stable and reliable system. The second UAV used was a Cheerson CX-20.

3.1.1.1 3DR X8+

The 3DR X8+ was the first UAV used in this research. It was used for the first and second prototypes as the base UAV. The X8+ was a powerful drone with a very good onboard flight controller i.e. the Pixhawk Autopilot System and it already came with components that were being used for the experimentation. The GPS module of the X8+ was another reason for choosing the system. It came factory configured with the 3DR uBlock GPS and Compass system which was cost effective, easily replaceable, and highly reliable. The X8+ is a commercially available, ready to fly, robust system with the real-estate to let us deploy multiple components on top of it. There was enough space on the drone's body to add components like the two cameras and the Raspberry Pi 2 on it without running into any load, balance or other issues. The X8+ was an expensive system and was mostly responsible for the ultimate price tag of the whole system. The only downside of using the X8+ was that its flight time on one battery charge was roughly 15-18 minutes. This made flying the UAV slightly risky, with loss of power and crashing being valid concerns. But with the Pixhawk's inbuilt Return to Launch Site and Land Safely functionalities, the drone loss rates could be minimized. The X8+ gave us a range of up to 100 meters when geo-fencing was enabled. For experimentation, those were the limits of our test range as well because of FAA regulations [8]. The X8+ is capable to lift a payload of up to 1 Kilogram with minimal effects on the flight time and stability. The X8+ has 8 propellers, working in tandem on four arms of the UAV. This gives the UAV extra load carrying capability as well as stability which is very useful in harsh weather conditions [6].



FIGURE 3. 1 3DR X8+ OCTO-COPTER [6]

3.1.1.2 *Cheerson CX-20*

The Cheerson CX-20 provides for an affordable UAV platform that can be used to carry medium range loads for photography and other purposes. This UAV of Chinese origin is light weight and agile, which makes it a good candidate for our project. It was easily able to carry the payload with minimal issues, though harsh winds did hinder its flight and some crashes were recorded. It has a flight time of approximately 15 minutes which is ample time for running tests. Its telemetry radios allow for a range of up to 300 meters which is more than what we could fly it at, given the line of sight restrictions. The CX-20's flight controller and GPS module gave performance comparable to that of the 3DR components, and it was also available with an open source license, therefore integration with the available code was simple [8].

3.1.2 Onboard Computers

The project employed use of two onboard computers. The main component of this whole research was the first onboard computer called the Raspberry Pi 2 while the other was a ready to use hardware component called the Pixhawk by 3D Robotics.

3.1.2.1 *Raspberry Pi 2*

The Raspberry Pi 2 is an easy to use, compact sized, single-board computer that is very cost effective. The chip costs around \$35 and has an ARM Cortex-A7 based quad core processor which is capable of running at 900MHz. The Pi has an internal memory of 1Gbytes which is impressive for the size. The Pi is capable of running a wide range of Operating Systems including Windows 10, but is primarily used for running Linux. The Pi's own operating system, the Raspbian, is also based on Linux and makes the use fairly simple. These were the main reasons for choosing the Raspberry Pi 2 as a candidate for use in this research. The Pi also weighs only around 50 grams which also played in its favor as an onboard computer for a UAV based system, since weights of components play a huge role in stability. The Pi can be run using a battery pack which was neatly attached to the UAV. With some work, the Pi could also be made to use the same battery as the UAV but this was avoided since flight times would have been affected.

The Pi provides multiple hardware interfaces which made integrating different components with it simple and provided us with maximum flexibility. A 10Gigabit Ethernet interface can be used for connecting to the Pi as well as a USB Wifi dongle for wireless connection. The Wifi dongle can be connected to one of the four available USB 2.0 ports. The Radio Antenna used in this research, for communication with the Ground Control Station, the Xbee Pro 900, was also connected to the Pi using a USB 2.0 port. A 40 pin expansion header is also provided on top of the Pi which provides 27 GPIO pins 3.3V, 5V and Ground supply lines for serial connectivity. This header was used to interface the FLIR Lepton camera with the Pi. The 15 pin MIPI Camera Serial Interface supplied on the Pi was used to connect the Raspberry Pi Camera Module. A micro SD memory card slot is also available which makes formatting and editing things on the memory as simple as taking the card out and connecting it to your computer [9].

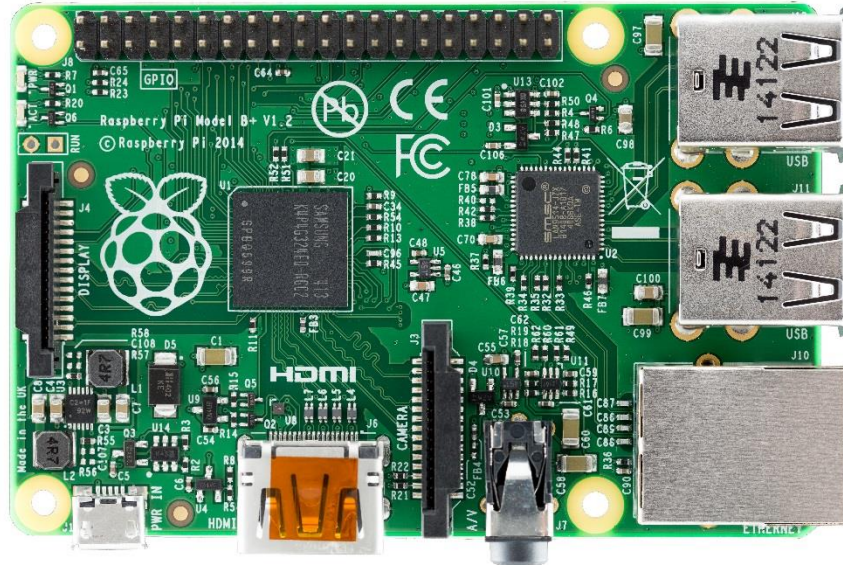


FIGURE 3.2 RASPBERRY PI 2 [9]

3.1.2.2 3DR Pixhawk Flight Controller/Autopilot System

The 3D Robotics Pixhawk Autopilot System is an integrated flight controller system that comes as a vital part of the 3DR X8+ UAV. This computer is responsible for all the flight controls of the X8+, including integration with the GPS and Compass system. The Pixhawk provides vital flight information which can be used in many ways. That was the main reason we connected to the Pixhawk and extracted information that was later used to categorize the images captured. The Pixhawk provides the GPS co-ordinates, altitude, compass heading, air-speed, angle of attack and other such information which has been used in this research. This information is vital to determining the location of a detected victim in a disaster situation. Details of the functionality are discussed in section 4.2.

The Pixhawk enables users of X8+ to fly the UAV using a Radio Control Transmitter/Receiver which interfaces with the onboard Pixhawk computer using 3DR Telemetry Radios [10]. The Pixhawk makes use of the ArduPilot Firmware for controlling the UAV and the related components in the Pixhawk suite e.g. the uBlock GPS system with compass.



FIGURE 3.3 PIXHAWK [10]

3.1.3 Cameras

In this research, we used two different cameras for capturing images on the ground. The primary camera, which makes the basis of this whole research, is the FLIR Lepton Thermal Camera, which is the most essential hardware component used. The other camera used was the Raspberry Pi 2's own camera module which gives color images at high resolution. Both these cameras were attached to the belly of the UAV at similar angles of view, giving us a fairly similar Field of View, even though the resolution of both the cameras differed drastically.

3.1.3.1 FLIR Lepton Thermal Camera

The FLIR Lepton camera is a compact, uncooled, long wave infrared sensor that provides a resolution of 60 x 80 pixels. This is a drawback of using this camera but we made changes in the deployment model of the UAV system which compensates for the shortcomings to some extent. The Lepton has temperature sensors on the housing and sensor base that can be used for telemetry purposes. It communicates over I2C and SPI ports, where I2C channel is utilized for configuration and commands while SPI channel is used for transferring frame data.

Although the output resolution is small, it gives out relative temperature readings instead of color pixels so we exploit housing temperature and sensor temperature to derive approximate temperature values in the given frame as an 80 x 60 matrix. The details of the approach for using this thermal image matrix is given in section 4.2.

Two models of the FLIR Lepton were used in this research project, making for the main difference between the first and second prototypes. Following Table shows a comparison between the two models of Leptons.

Feature	Lepton 50° FOV	Lepton 25° FOV
Camera Model		
Zoom	No Zoom	2x Zoom
Resolution	60 x 80 Active Pixels	60 x 80 Active Pixels
Field of View	50°	25°
Shutter (for Flat Field Correction)	Yes	No

TABLE 3.1 FLIR LEPTON CAMERA MODELS [11]

3.1.3.2 *Raspberry Pi Camera Module*

The Raspberry Pi Camera Module is a simple color camera with a resolution of 5 megapixels. The camera is compact in size; the whole camera along with the breakout board can be as big as the size of a quarter Dollar coin. The camera can be integrated with a Raspberry Pi 2 very easily using the 15 pin MIPI Camera Serial Interface [12]. The camera is by the same vendor therefore there are no issues about software or hardware compatibility. It is also capable of recording videos at a high definition resolution of 720p and an aspect ratio of 16:9.

The Raspberry Pi Camera has been used in this project so that real life images can be recorded in parallel with the thermal images. This can make familiarization with the terrain fairly simple and easy for the operators and rescue workers. The only strict “rule” for this camera’s deployment is that it needs to be attached to the UAV at exactly the same angle so that both cameras are looking at the same frame. The contents of the images can vary due to the difference in the fields of view of both the cameras but it still narrows the difference down.

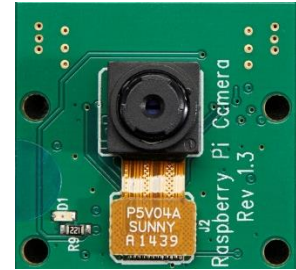


FIGURE 3. 4 RASPBERRY PI CAMERA MODULE [12]

3.1.4 **Radio Antennae**

We made use of two types of radios in this project. The first type were the telemetry radios that were part of the Pixhawk Auto Pilot system therefore we are just going to mention them briefly. These radios gave us basic connectivity between the UAV’s flight control system and the manual controller on the ground that the operator used. The second type of radios used were the Xbee Pro 900. These are telemetry radios that we customized for use on the transmission and reception of data.

3.1.4.1 *Xbee Pro 900*

The Xbee Pro 900 radios are configured with Digimesh firmware that allows for mesh networking between multiple radios, enabling our system to have an inter-UAV mesh for long range mesh deployment. The radios are equipped with 2.1dbi omnidirectional antennas to ensure signal propagation is uniform in all directions. This is a winning point for the use of these radios since unidirectional antennae would have made data transfer between the Ground Control and other UAVs almost impossible. Theoretically, the Xbee Antennae have an outdoor, line of sight range of up to 9 miles (15.5 km) at 100Kbps and 4 miles (6.5 km) at 200 Kbps [13]. This was found to be true in our limited range testing but could not be verified due to the FAA regulations.

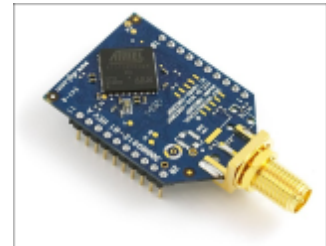


FIGURE 3. 5 XBEE PRO 900 [13]

We opted not to use high gain antennas since that would be detrimental in coverage if the UAVs aren’t flying in predetermined formations, which is the case in this work.

3.1.5 Others

In this section we talk about other relevant hardware components used over the course of this project that enabled us to get the end product and to fully utilize the rest of the major components to the fullest of their potential. The 3DR uBlock GPS and Compass module is one such component. This component enhanced the functionality and usability of our UAV system.

3.1.5.1 3DR uBlock GPS with Compass

The uBlock GPS and Compass module comes factory installed with the X8+ UAV but it is worth mentioning here since it plays a very vital role in the usability of the UAV system. The uBlock GPS module is used for geo-fencing purposes as well as functions like the Return to Launch and automatic landings [14]. It is also used by the UAV's own Ground Control Software to locate the UAV, create flight paths, assign flight missions based on waypoints and much more.



FIGURE 3.6 EXTERNAL, INTERNAL TOP AND BOTTOM VIEWS OF UBLOCK GPS MODULE [14]

In addition to all of those essential uses, we employ this GPS module for geo-location of survivor detection events. Whenever an image is captured on the cameras on the Pi, secondary information is also attached to it. Among this secondary data, the most important is the GPS Coordinates of where the image was captured and what the Compass heading of the UAV was at that exact time. These two factors can narrow the area of search down phenomenally and improve the rescue capabilities manifold.

3.1.6 Prototypes

In this section, we will talk about the different prototypes of the UAV that we deployed for Person Detection.

The first two prototypes differ only in that they used different modules on top of the same UAV system. The modules have been discussed in great detail in sub-sections 3.1.1 through 3.1.5 of this Chapter. The third prototype made use of a totally different UAV platform upon which the same hardware components as the second prototype were installed. We go into the relevant details of each prototype and discuss the components used and refer to questions like why the changes were made.

A. Prototype A

Prototype A was the first prototype deployed for the purpose of this research. It was based around the 3DR X8+ UAV platform. The major components used in this prototype were the Raspberry Pi 2, FLIR Lepton 50° FOV Camera, Xbee Pro 900 Radios, and Pixhawk for flight controls. The Pi camera was not used for experimentation in this prototype. There were some shortcomings in this prototype in terms of performance as the Lepton model did not give satisfactory results and operations were limited because of the limitations of the camera. Results from tests run using this prototype have been included in Chapter 5 for comparison purposes. Test plans also lacked detail when testing with this prototype, leading to further poor performance. This prototype was used mostly for creating a base case upon which further models were based. The code bank used in this prototype also lacked maturity which led to a lot of false positives.

B. Prototype B

The second prototype had a lot of improvements with the employment of a better camera; the FLIR Lepton 25° FOV gave far superior performance and allowed for higher altitude flights because of its 2x zoom property. For this prototype, we also attached the Pi Camera Module in parallel to the Lepton, on the belly of the X8+, though it was not actively used for experimentation. At that time, it was considered a secondary camera meant to be used in the future.



FIGURE 3.7 PROTOTYPE B WITH ALL THE COMPONENTS ATTACHED

This prototype proved to be very robust and was used in multiple tests in a range of different scenarios. These tests and scenarios are discussed in Chapter 4 and 5 of this document. This prototype tested our hardware knowledge as a lot of connections had to be made between the Pixhawk, the two cameras and the Raspberry Pi 2. This prototype for the first time in this research, made use of the uBlock GPS module as well, successfully attaching flight information to the images captured. This prototype made use of an external battery pack that was strapped onto the bottom of the X8's own battery pack on the bottom side of the UAV. This made for added weight that could prove a factor in destabilization of the system in harsh weather conditions. This problem was also mitigated in the third prototype. The installation of these components can be seen in detail in Figure 3.8.

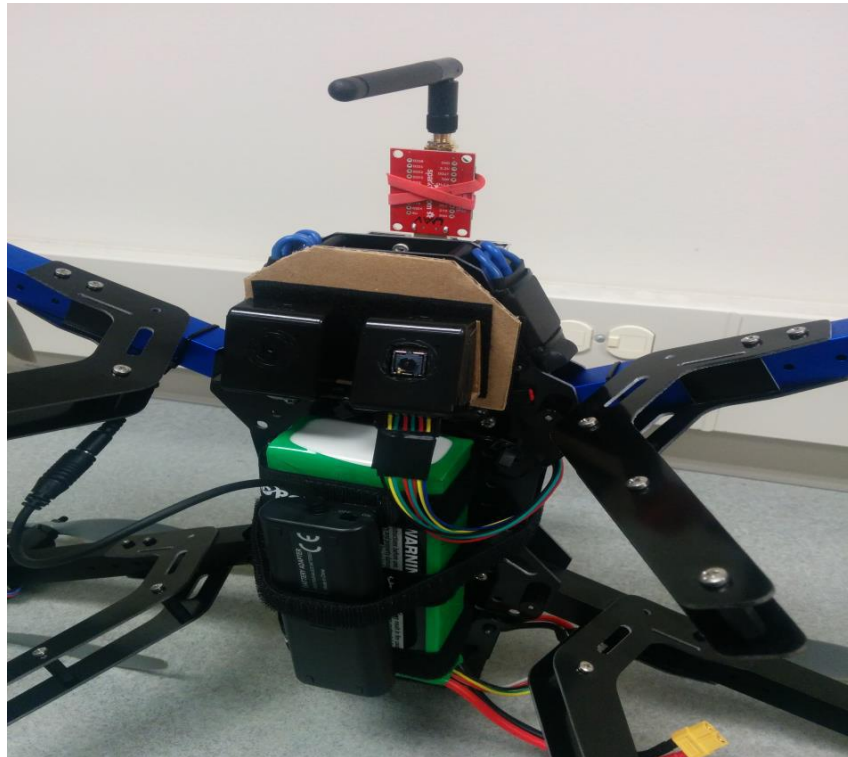


FIGURE 3. 8 PROTOTYPE B WITH FLIR LEPTON AND PI CAMERA MODULE INSTALLED

C. Prototype C

The third prototype turned out to be completely different compared to the first two, since the first UAV was lost in an accident and could not be recovered. This prototype made full use of all the hardware components mentioned in Sections 3.1.1 through 3.1.5. The main camera used for detection purposes was the Lepton 25° FOV with 2x zoom. Pi camera was also deployed in parallel as can be seen in Figure 3.9. The Pi camera, for the first time, was also used for capturing images in parallel and in synchronization with the Lepton. Both the cameras were installed at exactly the

same angles, which gave them the same angle of view. The only difference was caused due to the difference in the fields of view and resolution of both the cameras.

Another improvement was the use of a single battery for powering both the UAV and the Pi rather than two separate batteries. Some hardware modifications had to be made to facilitate the use of the UAV battery for powering the Pi. This gave this new, slightly lighter UAV more stability and made it less susceptible to harsh conditions.



FIGURE 3.9 PROTOTYPE C WITH THE REMOTE RADIO CONTROLLER

Table 3.2 gives us a comparison between the three prototypes and lists the main differences between each deployment.

Features	Prototype A	Prototype B	Prototype C
UAV	3DR X8+	3DR X8+	Cheerson CX-20
Raspberry Pi 2	Yes	Yes	Yes
Pixhawk	Yes	Yes	No (3DR APM 2.6)
FLIR Lepton 50°	Yes	No	No
FLIR Lepton 25°	No	Yes	Yes
Pi Camera Module	No	Yes (Limited)	Yes
Xbee Pro 900	Yes	Yes	Yes
uBlock GPS	Yes	Yes	No (uBlock Neo-m8n)

TABLE 3.2 COMPARISON OF PROTOTYPES

The following diagram shows the relation between all the hardware components and how they communicate with each other and how data is transmitted to the Ground Control Station. The arrows in the diagram indicate information flow while the protocols/physical mediums used for interfacing between devices are also shown at each link. Once all the data is collected by the Raspberry Pi 2, it is packetized and sent to the Xbee Pro 900 radio onboard the UAV which in turn sends it to the Ground Control Station.

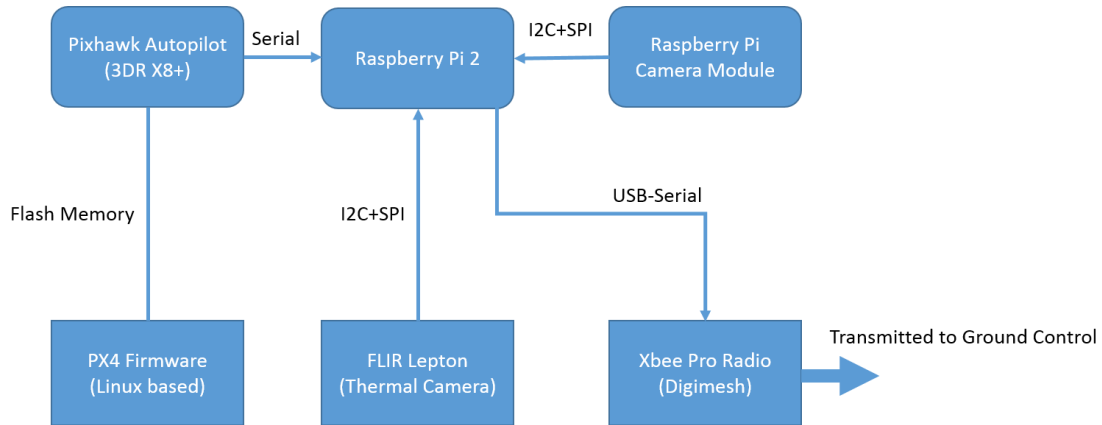


FIGURE 3. 10 HARDWARE ARCHITECTURE (UAV)

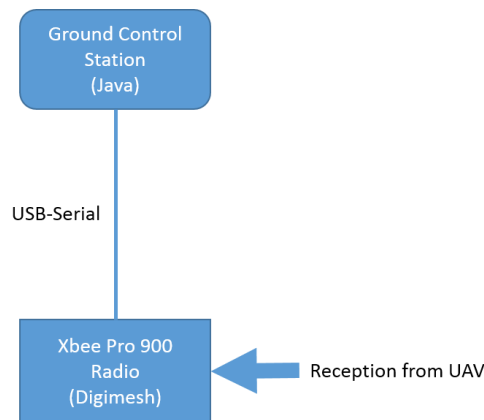


FIGURE 3. 11 HARDWARE ARCHITECTURE (GROUND CONTROL STATION)

As shown in the above figure, the Ground Control Station makes use of a single Xbee Pro 900 radio for communicating with the UAVs. This use of a single radio leads to the design of a circular buffer technique that we used in order to deal with the problem of communicating with multiple drones at the same time.

3.2 Software Design and Architecture

The software design consists of a number of modules implemented in Python, Java and C languages. The software components are divided into two categories; the system that is running onboard the UAV and the system that is running on the Ground Control System. The following figure shows a detailed look at the components of software architecture of this system.

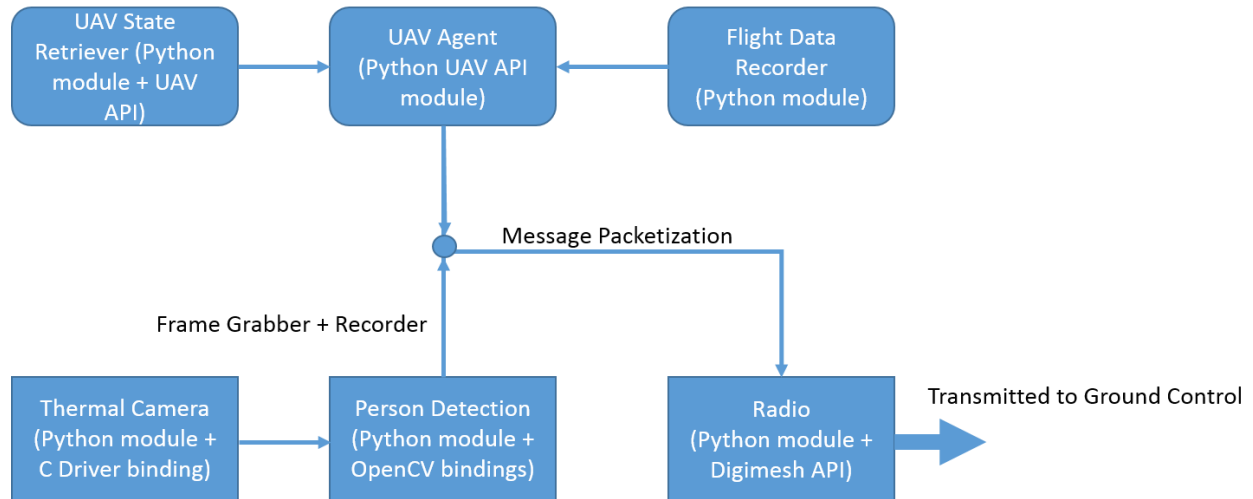


FIGURE 3. 12 UAV SOFTWARE ARCHITECTURE

3.2.1 UAV based Software Architecture

In the above figure, the UAV Agent is the principal module that runs under Drone API [16]. This in turn is a process running under the MAV Proxy daemon [17]. MAV Proxy is a middleware that communicates with the UAV using serial connection over MAV Link protocol. It provides the UAV's flight information with a rich Python API, the Drone API. This enables us to run the custom built UAV Agent module which uses multiple modules to capture thermal images from the Lepton, retrieve UAV information from Pixhawk, record frames and push them to the person detection module for classification and identification. Once that is done, messages are created in packetized form with all the information attached, ready to be transmitted to the Ground Control Station using the Ground Communication network between the UAV and the GCS.

The Thermal Camera module comprises of two layers. The first is the lower layer which consists of a custom built device driver written in C. This driver captures thermal frames and temperature readings from housing and core sensors. The second layer is the Python module that interacts with the device driver over Python-Ctypes bindings and retrieves frame data in an

OpenCV supported matrix format along with temperature sensor readings. The Thermal Camera module has a recording functionality built in that records these raw frames and readings in a text file twice every second (2 FPS). Matrix data is in uint16 format and is base64 encoded when written in the recording file. The UAV Agent retrieves thermal frames once every two seconds (0.5 FPS) using the Frame Grabber submodule and feeds it to the person detection module along with UAV state information (person detection module requires UAV altitude data).

The detector module makes use of Hot Spot Classification technique to identify people on ground as individual blobs [15]. Before this classifier executes, the thermal frame is threshold using a combined low-pass and high-pass filter retaining temperature values falling between average human skin temperature and thermal sensor's housing temperature a.k.a. the environment temperature. After this pre-processing step, MSER hot spot identification is performed using the OpenCV MSER module. The output from MSER is a set of blobs [18], which are then post-processed based on UAV altitude and an average person's surface area in the captured frame.

We observed that given our thermal sensor has a field of view of 25° and that it is oriented laterally. This means that increase in the UAV altitude reduces thermal signature of a person in terms of blob size in the frame. We exploit this relationship to filter out noise from the frame and keep only blobs with high probability of identifying a person on ground. After that, depending on whether the environment temperature was higher than or lower than average human skin temperature, we extract coldest or hottest blobs respectively from the frame. If there is a non-zero number of these blobs, we flag them in the frame and classify the result as a positive of people being present on ground at the relative locations where the specified blobs (hot spots) are found.

The result from detection is combined with UAV's flight state information and messages are generated to be sent to other UAVs and the Ground Control Station. The message broadcasted to other UAVs on a 1-hop radius does not contain the actual frame data and only contains flight data. In contrast, the message that is unicasted to the GCS contains the image as well as the flight data. This helps in keeping all UAVs coordinated and GCS aware of the detection results and frame images. Before being sent, the message directed to GCS is written to flight recording file. This is the job of the Flight Data Recorder, which serves like a black box in airplanes. Frame data is byte64 encoded and the entire message is JSON packed on which gzip compression is applied. The frame data is not transmitted in raw matrix format, but it is first rendered into a JPEG image (80 x 60 resolution) and the JPEG compression level is adjusted based on the RSSI of the radio, in order to make the system resilient in low signal strength conditions. This means that the lower the RSSI, higher the JPEG compression. If the RSSI falls too low, frame image is omitted altogether and the rest of the data is packed into the message.

The Radio module is responsible for packetization of messages and transmission to the GCS and peer UAVs. UAV Agent sends packed messages to Radio module which fragments them before sending. The Xbee Pro radios have an MTU of 100 bytes and the average size of message is 7-12Kb (depending on JPEG compression). Therefore, to transmit these messages, they need to be fragmented into chunks of 100 bytes or less, which are then prepended with sequence numbers to be assembled properly at the receiver.

3.2.2 Ground Control Station based Software Architecture

The Ground Control Station is a Java application that incorporates GIS maps and connects with Xbee radio over USB-serial connection. It uses Digi's Java API for Xbee radios to receive and send messages (JSON messages). The GCS receives message fragments from the UAVs and has per-sender buffers to gather fragments and assemble messages. The received messages contain UAV flight information (GPS co-ordinates, heading, airspeed, groundspeed, altitude) and thermal image along with detection results. UAVs are rendered on the map based on their coordinates and the flight path is also drawn.

The GCS is also responsible for time-synchronization of UAV onboard Raspberry Pi's since Raspberry Pi doesn't come with a real-time clock. To achieve that, the GCS periodically broadcasts current time over the mesh network and the UAV Agent module running on the Raspberry Pi synchronizes the system clock based on the received timestamp. This process does result in a slight clock drift between UAVs and the GCS but it is well under a second, which isn't critical for our application.

An important improvement made to Prototype C in terms of software design is that it is fully capable of recording pins of locations where person detections have been made. These pins are placed on a map for easy visibility and easy categorization of results and reports. Another improvement is that for all the captures, both thermal as well as color captures, a detailed log is maintained in .csv format. This log maintains a record of each capture file reference name, along with the timestamp (which also includes the date), GPS co-ordinates, altitude, heading, air and ground speeds of the UAV and the RSSI of the radio at that particular instance. Logging all of this information is vital to the performance of the system as these logs can be later referenced to verify records and to provide accountability for the UAV's operations. A sample of this log can be seen in Appendix A of this document.

3.3 Deployment Architecture

According to Murata et al, the disaster search and rescue operations can be classified into three different categories [19], as shown in Figure 3.13.

Wide Area search is usually carried out using large planes flying at high altitudes, with high resolution imaging systems that can assess the overall situation in a disaster struck area. This can also categorize areas for the other two types of search and differentiate between areas that rescue efforts can be started in and areas that cannot or should not be accessed just yet due to damages and susceptibility. The second type of search is the Narrow Area search that can be carried out by hovering crafts like Helicopters or large remote control drones. This further narrows down areas for rescue teams on the ground and focuses mainly on the areas of interest pointed out by the cursory wide area search. The third and final type of search is the pinpoint search which is

carried out on the ground by personnel and takes the most time. This type of search can also be very hazardous if proper steps are not followed.



FIGURE 3.13 THREE TYPES OF RESCUE OPERATIONS [19]

Our system can be placed between the second and third search types, and can be called a hybrid of both. Our system is UAV based and covers large areas compared to personnel on the ground, with a wider field of view, therefore it has characteristics of the narrow area search process. At the same time, since the altitude is not very high, it has a far more detail outlook on the situation, which is a characteristic closely related to pinpoint searching. Our system can also pinpoint locations of survivors based on thermal images, GPS co-ordinates, air speed and heading information. Our system is also avoids life threatening situations which on ground searches at initial stages of a disaster can't guarantee. This makes our system ideal for use in the field.

Our UAV based person detection system can be deployed as either a single unit system where only one UAV is flown that gathers information over a small geographic area, or it can be launched in a mesh formation with multiple UAVs flying as a swarm.

The single unit deployment can be used for pinpoint searching in narrow areas where quality (accuracy) is of more importance compared to quantity. This type of searching would take a far longer time though, due to the limited flight time of our prototypes and the limited field of view of the cameras.

To counter this, the swarm deployment can be used where multiple UAVs fly in a formation. According to Figure 3.14, the network is divided into two mutually exclusive components, the inter UAV network and the ground communications network. The ground

communications network works in the similar way as the single unit deployment but the inter UAV network is used for communication and co-ordination between the swarm of drones. Mesh functionality is already available with the Xbee Pro's DigiMesh firmware.

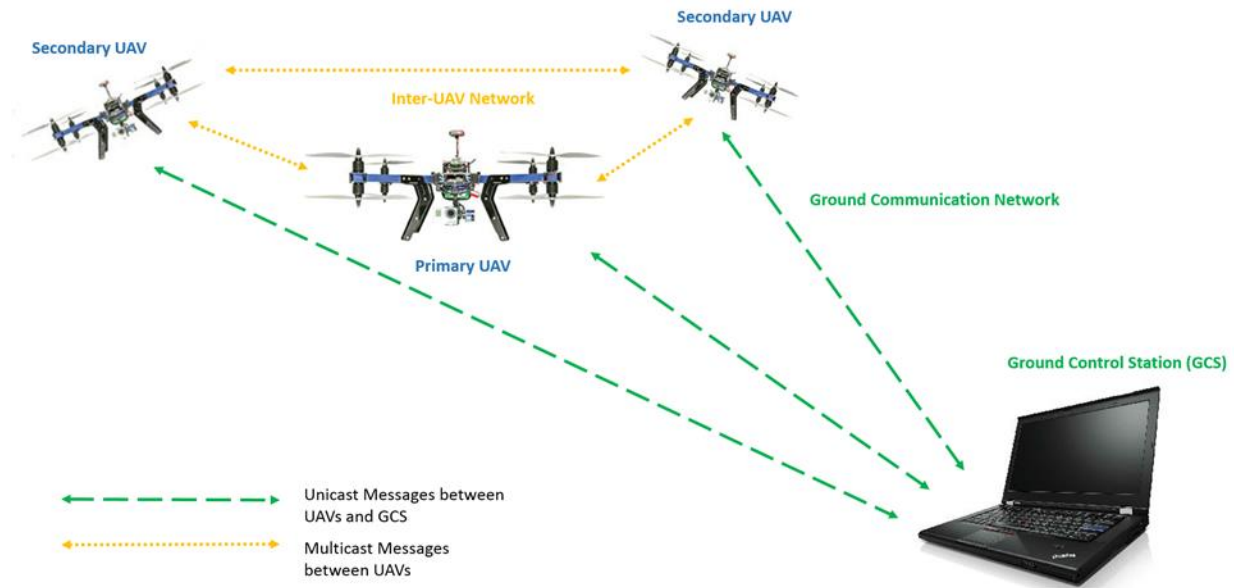


FIGURE 3. 14 MULTI UNIT DEPLOYMENT WITH A MESH NETWORK

This mesh deployment is favorable in many ways. For example, it provides redundancy, since if one UAV goes down, others can take over and not let the mesh break, not compromising the mission. On the other hand, it also provides for the ability to scan large areas in minimal time. This is very important as it would save precious time in a disaster situation.

Chapter 4

Experimentation

In this chapter, we discuss the details of the test plans devised to test the functionality of this system. This chapter also goes into the details of how each experiment was carried out and the significant moments in each and every experiment.

4.1 Environmental Metrics

In order to be able to gauge the performance of the system, a number of test scenarios were devised. These test scenarios would help us test the actual capabilities and limits of our system. These tests also gave us the capability to determine the system's optimal operational values. These test cases are discussed in Section 4.2.

For the test cases to be successful and for us to be able to measure the performance, some environmental metrics had to be designed. These metrics are listed as follows:

4.1.1 Scenarios

For our tests, we focused on two types of disaster scenarios. These were simulated while our tests were being conducted. These two scenarios formed the basis of our experimentation as all the other metrics were connected to these. The two scenarios we tested for are:

- Earthquakes

- Floods

Since the primary focus of this study is on natural disasters, we decided to simulate the two most common and devastating disasters where the system could be utilized to the fullest of its potential. We had to exclude many other common scenarios like Hurricanes, Typhoons, and Wild Fires etc. due to the limitations of our system. Since we are using a thermal imaging sensor, the system would fail to give any conclusive results in a scenario where large fires are included. At the same time, scenarios like Typhoons and Hurricanes were also excluded as the system is supposed to be deployed in the immediate aftermath of a disaster and these kinds of disasters have properties like rains and high winds associated with them which would render our system unstable and cause it to crash. It should be noted that our system can be deployed in water related disasters and it can be used to some extent in Hurricane situations, though after the winds have subsided. Tsunamis are not explicitly named here as they are considered as a form of floods for the sake of this research.

4.1.2 Altitudes

The altitude of the UAV plays a very important role in the accurate detection of humans on the ground. For the first prototype, since we were using the first model of Lepton, we had to fly at lower altitudes since the image quality was deteriorating immensely. With the introduction of the second model of Lepton in Prototype B, we saw that the zoom quality of the lens gave us the ability to fly at higher altitudes without compromising the quality of images that much. We also saw that at previous altitudes, the image quality was enhanced manifold. For this reason, we chose a number of ranges to fly in. The lowest altitude we flew the system at was 5 meters while the highest we went while the cameras were running was 40 meters. At 40 meters, the images started to turn into one large blur and no detection could be made. We list the altitudes at which the experiments were conducted as follows:

- 5 meters
- 10 meters
- 20 meters
- 30 meters
- 40 meters (max)

4.1.3 Weather Conditions

As we have mentioned in the previous sections, our system at the moment, is not all weather capable. This means that the tests had to be arranged in weather conditions that were favorable to the safety and functionality of the system. Keeping that in mind, we still wanted to test the versatility of the system therefore we decided to execute the tests in different conditions. These conditions were simulated based on the test subject's location on the ground. The test subjects were placed in two contrasting states; in some tests they were placed under a cool shade while at other times they were detected in sunny conditions. In sunny conditions, the dynamics of detection

change and the thermal camera's abilities are slightly waned. This is because of the fact that surrounding environmental temperatures rise, increasing the possibility of false positives. As mentioned before, the system is not waterproof therefore it could not be used in rain. Prototype A and B, with the use of the X8+, proved to be very stable even in windy conditions and some tests were executed on days when there was a high side wind on the flight path of the UAV. On the other hand, the CX-20 proved to be less stable in windy conditions and therefore operations for Prototype C are not recommended in high wind situations.

4.1.4 Time of Day

Our system features the use of a thermal imaging system, which means that it can very easily be used in any kind of light conditions. In fact, the system works much better when there is low light in the surrounding environment as then the ambient temperatures of the surroundings are low and person detection can be done with higher accuracy. Tests were conducted at different times of the day, ranging from anywhere around noon to late afternoon and even evenings. For the Time of Day metric, we split the tests into two distinct values; Day time and Night time.

4.1.5 Surface Type

Another metric that is of paramount importance when it comes to determining whether or not the system would be effective in a real life scenario is the surface type upon which the test subjects are located. Surface type can have a positive as well as negative impact on the results as different types of surfaces have different reflective and conductive qualities. Some surfaces, like roads, tend to be less reflective but can absorb a huge amount of heat during day time. This can have a negative impact if the test subject is present in close proximity of the road surface. Similarly, if the test subject is standing in a grass filled piece of land, his or her heat signature would be far more superior in quality compared to the surrounding, making him/her stand out and easily detectable. For our tests, we took into consideration three types of surfaces, namely, Asphalt/Concrete, Grass and Water. Asphalt and Concrete have been listed together since they proved to be of similar quality when it came to their heat signature. Water, due to its reflective nature, gave us faulty readings, though detection was made successfully at high rates. For flood simulations, we made use of the local swimming pool with test subjects partly submerged in the water.

4.1.6 Movement

Movement of the object and the UAV have a huge impact on the rate of detection. Movement is a metric that is measured in terms of the relative motion of the UAV in comparison to the test subject and vice versa. We took into account three different combinations of movements for our experiments. In the first case, we had the UAV fly over a stationary test subject. This fly-by movement model proved to be very successful at slow and medium speeds, and gave us the

second best results. The second movement case was where the UAV is stationed immobile at a predetermined altitude and heading, while the test subject moves towards and away from the UAV. This motion case was also successful to some extent, though the results were not as conclusive as the other two cases.

In the final case, which could be considered as the base case for all the experiments, we used a stationary UAV looking at a stationary test subject, while altitude of the UAV was altered. This proved to be the most successful case as results were very productive.

A fourth case was also observed, where both the UAV and the test subjects were moving relative to each other, either in the same direction, or opposite to each other, but that case was highly inconclusive due to high speeds.

4.1.7 Test Subject Profiles

The physique of a test subject would also play an important role in the experimentation and data gathering process, since every human has a different cross section on a camera frame. Therefore, it is necessary to talk about the test subjects who volunteered for this research.

Test Subject A was a 26 year old, 6 feet tall male of lean physique. He was the main subject for most of the Prototype A and B tests.

Test Subject B was a 19 year old, 5 feet tall female with lean physique. She was employed for tests conducted at the swimming pool for the flood scenarios.

Test Subject C was a 14 year old, 5 feet tall male with a normal physique. He was employed primarily for testing with Prototype C.

The test subjects were asked to be positioned in different postures. These postures were categorized as Prone, Crouching and Standing positions. The test subjects were also asked to increase their surface area and signature by spreading their limbs. This was only done in the on-ground tests and not in the water tests. Results vary for different positions and profiles.

4.2 Test Plans

A number of test plans were created, in order to systematically test the limits of our system. This section talks about these test cases and discusses each case in relevant detail. For this document, since we have discussed the first Prototype in detail, even though the results were highly inconclusive, we will include it and discuss the test cases and results as they formed the basis for the whole research. This sub section looks at each Prototype and the tests conducted with them separately.

A. *Prototype A*

Prototype A was highly experimental, and most of the equipment used was yet not being used to the fullest of its potential. Therefore, the test cases were not very polished either. Due to the lack of former operational knowledge, the test cases were not sophisticated and had to be conducted on mostly ad-hoc basis.

In testing for Prototype A, we considered a small number of metrics. These primarily included the scenario of Earthquakes. Altitude of the UAV was set at approximately 10 meters. The speed at which the UAV passed over stationary subjects was set at 2 miles per hour. Test subject A was employed for these tests and simple scenarios were tested. Surfaces involved in these tests were Grass and Asphalt while all the tests were conducted at day time.

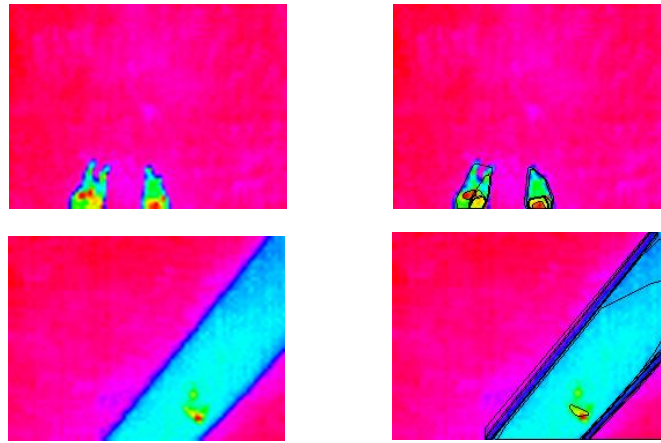


FIGURE 4.1 IMAGES CAPTURED WITH PROTOTYPE A, WITH MSER BLOB DETECTION

In the above images, we can see that the blob detection algorithm that is run on the images and the software detects the temperature blobs inside the images, encircling them in thin black lines.

These tests, however, were primarily inconclusive due to the lack of operational knowledge as well as lack of high quality equipment. The 50° FOV Lepton failed to give good results, which led to the adoption of a completely new prototype.

B. *Prototype B*

For Prototype B, a number of Use Cases were created, following which much better results were acquired. The Environmental Metrics involved in these tests can be seen in detail in Table 4.1.

	Metric	Prototype A	Prototype B	Prototype C
Scenario	Earthquake	✓	✓	✓
	Floods	✗	✓	✗
Time of Day	Day	✓	✓	✓
	Night	✗	✓	✗
Altitude	5 m	✗	✓	✓
	10 m	✓	✓	✓
	20 m	✗	✓	✓
	30 m	✗	✓	✗
	40 m	✗	✓	✗
Weather Conditions	Sunny	✓	✓	✓
	Shade	✗	✓	✓
	Rain	N/A	N/A	N/A
Surface	Asphalt/Concrete	✓	✓	✓
	Grass	✓	✓	✓
	Water	✗	✓	✗
Movement	Both Stationary	✓	✓	✓
	Moving UAV	✓	✓	✓
	Moving Subject	✗	✓	✗
Test Subjects	Person A	✓	✓	✗
	Person B	✗	✓	✗
	Person C	✗	✗	✓

TABLE 4.3 PROTOTYPES AND RELEVANT METRICS

Since many tests were conducted for Prototype B, they have been categorized with relevant details as follows:

Test A

For the first test, we considered the scenario of an Earthquake, simulating a body lying on the ground. Test Subject A was asked to hold their arms and legs open so that their surface area and heat signature could be maximized and highly exposed to the camera. The test subject was located on a grass surface, in a shady area. The movement scenario simulated here was such that both the object and the drone were stationary. Images were captured at altitudes of 5, 20 and 40 meters, which can be seen in Figures 4.1 a, b and c respectively. As we can see, the images captured with this prototype are crisp, more detailed, and give much better results compared to its predecessor.

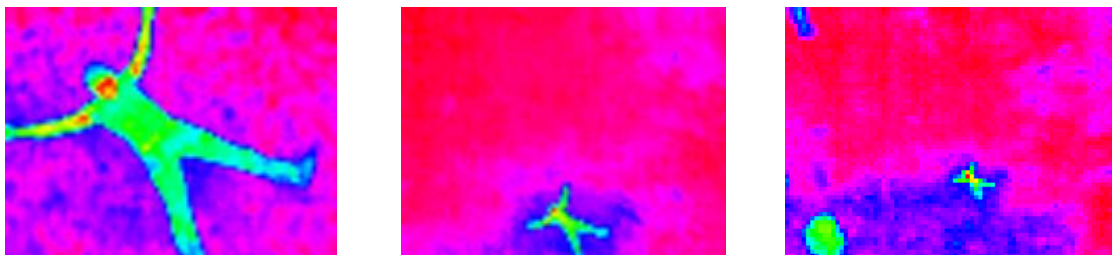


FIGURE 4. 2 A) IMAGE TAKEN AT 5 METERS B) SAME POSTURE AT 20 METERS, C) OBJECT VIEWED AT 40 METERS

Test B

The second test was carried out in the same environment. The test subject was asked to change their posture to the crouching position, effectively reducing their surface area and therefore, their heat signature area. Approximate change of the actual surface area was calculated at 4 square feet which was less than half of that of the previous test. The results can be seen in the images shown in Figure 4.2 a, b and c. In Figure 4.2 c, we can see three objects, with the test subject being the object at the top of the picture. The two blobs at the bottom are other people who were present in the vicinity while the blob to the upper left side of the image is a tree.

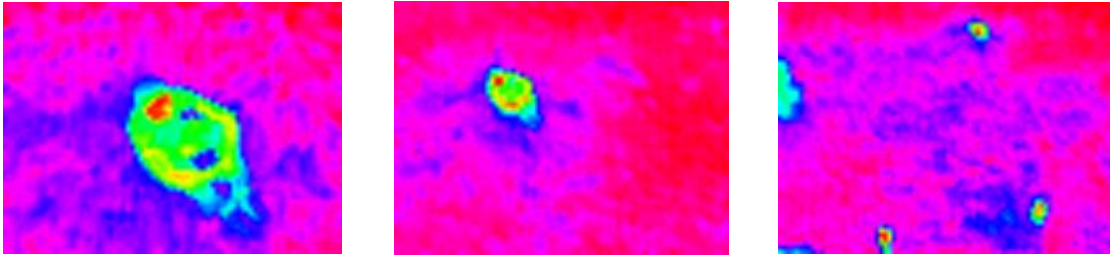


FIGURE 4.3 A) IMAGE TAKEN AT 5 METERS B) SAME POSTURE AT 20 METERS, C) OBJECT VIEWED AT 40 METERS

Test C

For the third test, the test subject was asked to stand with their arms held close to their body, on an asphalt path in the middle of a grassy patch of land. This was used to simulate earthquake affected people who are travelling on foot over various kinds of paths they might encounter. The effective surface area of the person was reduced, compared to the first test, but was slightly larger than the second test. Images, as seen in Figure 4.3, show that the person would be easily detected as their heat signature is clearly visible compared to the surroundings.

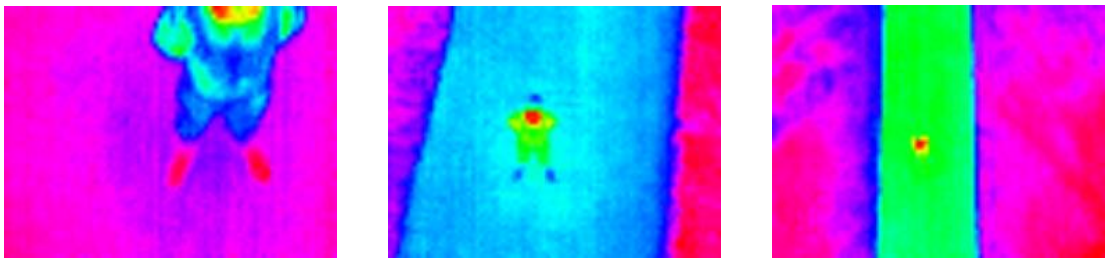


FIGURE 4.4 A) IMAGE TAKEN AT 5 METERS OVER ASPHALT PATH B) SAME POSTURE AT 20 METERS, C) OBJECT VIEWED AT 40 METERS

Test D

For Test D, the background environment was the same as Test C, except that the time of day setting was Night time and the test subject was asked to move at different speeds both towards and away from the stationary UAV. The UAV was kept stable at an altitude of 20 meters using the Loiter or Altitude Hold setting of the Pixhawk. This scenario was used to simulate detection of people moving around in disaster areas, which can be used for relief efforts as well as mapping

purposes. Figure 4.4 shows different images captured during the execution of this test. The test subject was first asked to walk away from the drone at a slow pace of 5 kilometers per hour. In the second instance, the test subject was asked to walk faster, at 7 kph, towards the drone. In the last instance, the test subject was asked to run away from the drone at 15 kph. Speeds were calculated based on the distance covered which was approximately 20 meters and the UAV camera was only looking at part of the 20 meter strip, to simulate limited area coverage during flight and so that the object could move in and out of the frame. In Figure 4.4 c, we can see that the UAV barely caught the object in the upper right corner of the frame, which is still enough to do detection.

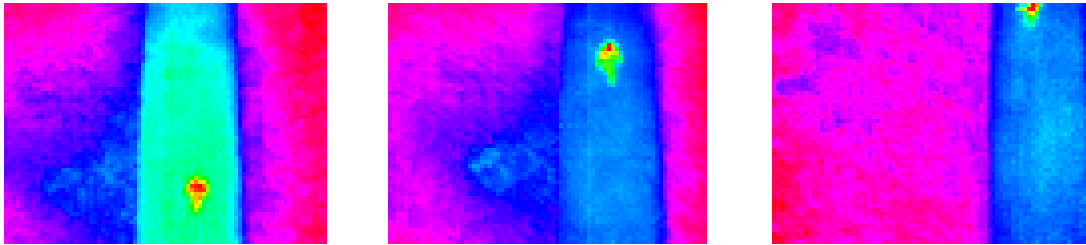


FIGURE 4. 5 A) IMAGE TAKEN AT 20 METERS WITH TEST SUBJECT MOVING AWAY FROM THE DRONE AT 5 KPH B) MOVING TOWARDS THE DRONE AT 7 KPH, C) RUNNING AWAY AT 15 KPH

Test E

Test E was carried out to simulate a moving UAV, covering a large area while object are stationary. For this test, the setup was kept exactly as it was in Test D. The only difference was that the UAV was moving at varying speeds of 1, 2 and 4 kph while the objects were kept stationary on an asphalt path. The images in Figure 4.5 show the different captures during this test. One problem encountered during this test was that since the Lepton camera was not meant to be used on a UAV, some of the images were very blurry and could not provide sufficient data for testing.

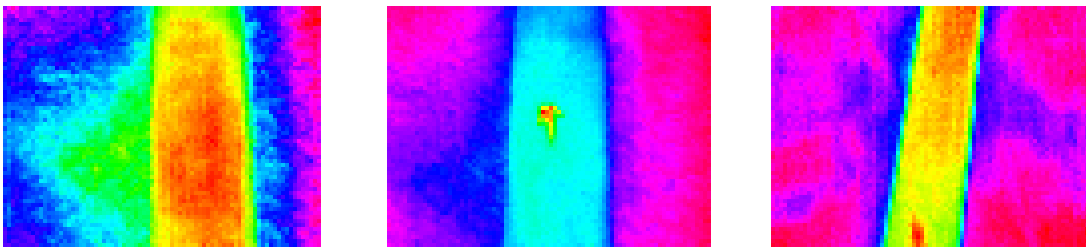


FIGURE 4. 6 A) IMAGE TAKEN AT 20 METERS WITH THE DRONE FLYING AT 1 KPH B) FLYING AT 2 KPH, C) FLYING AT 4 KPH

Test F

The final test for Prototype B was conducted at the public pool, to simulate flood conditions. Test Subject B volunteered and was asked to submerge half of their body in the water so that effects of the water and its reflection could be observed in the test. The results were surprisingly accurate with the camera capturing the submerged part of the body, even on a sunny day. The drone was flown at approximately 10 meters of altitude and was kept stationary. The test subject was also stationary and was at the edge of the pool. Figure 4.6 shows the results of the test.

In Figure 4.6 a, we can see the test subject in the center left of the frame while in 4.6 b, the test subject's submerged legs can be seen through water, at the upper right corner of the frame.

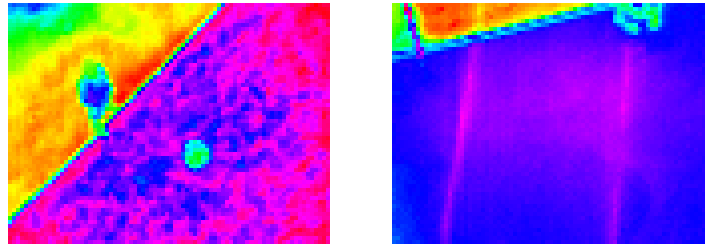


FIGURE 4.7 A) IMAGE TAKEN AT 10 METERS SIMULATING FLOODS AND B) SUBMERGED LEGS OF THE TEST SUBJECT SEEN

C. Prototype C

For Prototype C land tests were conducted to simulate earthquakes. Test Subject C was employed for testing this prototype. The tests were similar therefore they have been compiled into two separate categories and details have been distributed into sub-sections for better understanding.

Test X

This was the first test for Prototype C. In this test, subject C was asked to stand in a sunny location on a grassy surface at noon time. Due to the intense heat accumulated by the surroundings, the images give results that don't favor the subject much. Tests were conducted at maximum altitudes of just 20 meters due to harsh weather conditions.

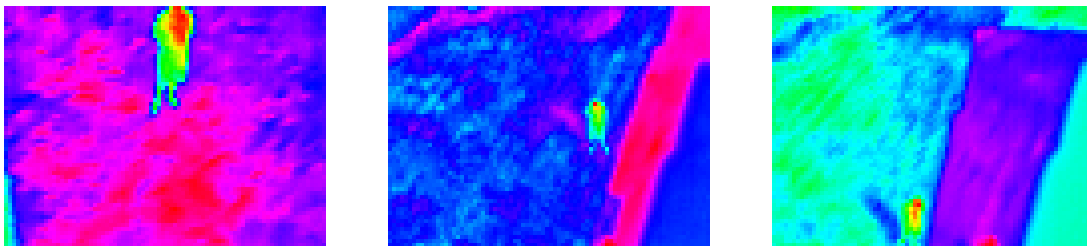


FIGURE 4.8 A) SUBJECT AT 7 METERS, B) SUBJECT AT 15 METERS AND C) AT 15 METERS WITH A SIDE DRIFT

As can be seen in the images, the test subject is visible in the first two frames with almost perfect accuracy but as the UAV gains altitude, the surroundings impair visibility and the shady part (purple strip in the third frame) superimpose on the subject's heat signature.

The test subject was also moved to the shady part of the test area, as can be seen in the images. The results vary phenomenally compared to the same altitude but difference in the location and shade conditions. In the third frame of Figure 4.7, a side drift on the UAV was caused due to high winds, which made the UAV move towards the right, changing the angle of view.

As mentioned in the detailed description of each prototype, we have a functional Raspberry Pi camera onboard Prototype C which is capable of capturing frames at exact times that the thermal images from the Lepton are captured. This add-on feature is used to further assist human operatives of the system since it is tough for humans to make environmental and geographical sense of the terrain from a thermal frame. Figure 4.8 shows the frames captured at the exact time when the thermal frames in Figure 4.7 were recorded.



FIGURE 4.9 A) SUBJECT AT 7 METERS, B) AT 15 METERS AND C) AT 15 METERS WITH A SIDE DRIFT

It is important to note that the color images are not exact replicas of the thermal images since the field of view and resolution of both the cameras vary immensely. Nonetheless, the cameras are both set up at same angles on the UAV so that there is minimal drifts in the images of both the cameras.

Test Y

For Test Y, the background was changed from merely grassy to asphalt. Multiple frames of the same test subject were captured at varying altitudes. Along with the thermal frames, color images were also captured using the Pi camera module. The resultant images are shown in Figure 4.9.

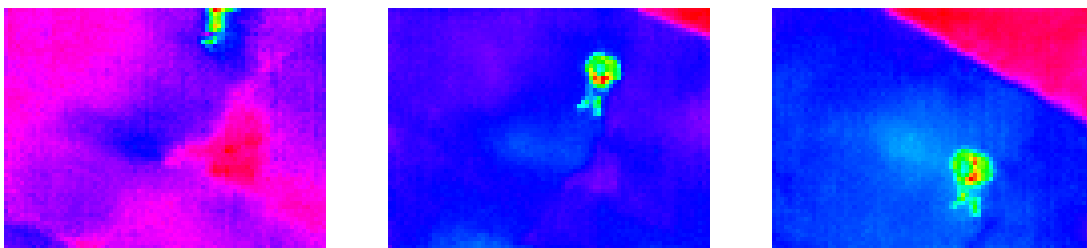


FIGURE 4.10 THERMAL IMAGES CAPTURED AT ALTITUDES OF 7, 12 AND 15 METERS RESPECTIVELY

For the same frames, color images that were captured are shown in Figure 4.10. We can see how clearly the high-contrast asphalt background makes the heat signature of the test subject “pop-up” and makes the subject highly visible.



FIGURE 4.11 COLOR IMAGES RECORDED AT ALTITUDES OF 7, 12 AND 15 METERS RESPECTIVELY

We can visibly observe the difference between the captures of both the cameras. Since the Lepton is the primary camera and is the focus of this study, when flying the UAV, we focus on the view point of the Lepton. Since it only has a much more focused field of view of just 25° , the Pi camera can sometimes miss the subject.

In contrast, sometimes the Pi camera perfectly recorded images of the test subject but the Lepton missed most of the capture and the test subject barely made it into the frame. The following example shows this anomaly of the system. This is caused because of the wide angle view of the Pi camera which can capture a wider area in a frame while the Lepton is much more focused and in comparison, can miss some spots.

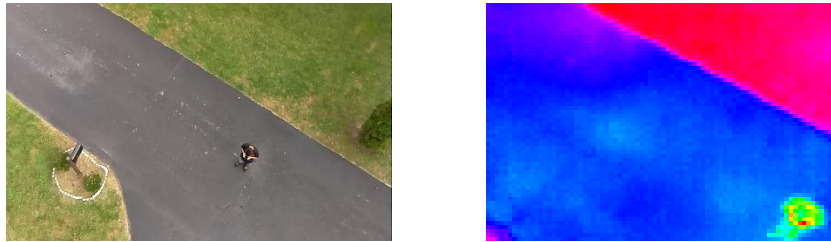


FIGURE 4.12 IMAGES CAPTURED AT AN ALTITUDE OF 12 METERS

In Figure 4.12, we can see that Test Subject C is perfectly centered in the first frame, which is recorded using the Pi camera, but the Lepton barely captured the subject in its frame. These anomalies have been seriously considered and it is believed that these issues can be resolved with the use of better thermal cameras with a wider field of view.

D. Results of Person Detection Algorithm

Following the capture of thermal frames, they are processed using the MSER algorithm. This algorithm is the main blob detection function of the system. The algorithm processes the images in two stages:

In Stage 1, the images go through initial person detection where the MSER algorithm engulfs each blob in the frame by a thin black line. This can be considered as the pre-processing

step of MSER as it forms the basis for the second stage. Sometimes, the images are so crisp and clear that a second stage is just left as a formality but at other times, the second stage is deemed necessary. We show the results of the first stage for some pictures shown in the above test plans:

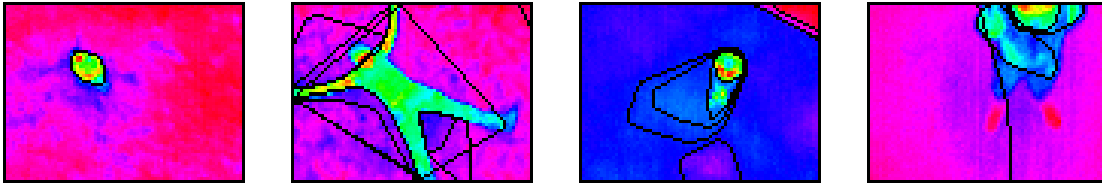


FIGURE 4. 13 MSER STAGE 1 APPLIED TO MULTIPLE FRAMES FROM DIFFERENT TESTS

We can see that the initial results are not necessarily satisfactory and a second pass needs to be made. In the first frame, a proper detection event is recorded even without the second pass but for the rest of the images, a second pass has to be made. It should also be noted here that sometimes, the subject's surface area can be broken into multiple blobs as can be seen in the fourth frame. This is due to the temperature differences in different parts of the body. This can lead to false multiple detections and void the results. This issue can be mitigated by flying the UAV at an altitude that is optimal for detection. A suggestion is made at the end of the next chapter regarding this issue.

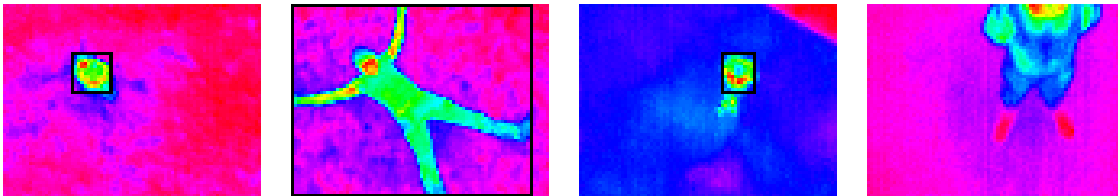


FIGURE 4. 14 MSER STAGE 2 APPLIED TO STAGE 1 FRAMES. NOTE THAT THE LAST FRAME SHOWS NO DETECTION AND MAKES A FALSE NEGATIVE JUDGEMENT.

We can easily see that the results of the MSER second stage are clearer with proper detections made. In the first frame, the person is perfectly detected and annotated. In the second image, even though the blob is of irregular shape, the MSER second pass recognizes it as a person and annotates the picture, triggering an alarm to mark the recognition. In the third image, we can see that the upper body of the subject is only considered as a blob but still the detection is true and leads to a true detection event. In the last frame however, we can see that the person is not detected due to multiple blobs present in the image. This can lead to many false negative events and many failed detections.

Results based on these detections are discussed in detail and categorized in Chapter 5.

Chapter 5

Evaluation and Discussion

In this chapter, we discuss the results of the experiments performed as described in detail in the previous chapter. We will divide the results into three categories, based on the prototype that is being discussed. Inside each subsection, we will discuss the details of different relevant metrics that were applied during testing of each of the prototypes. The metrics considered in this chapter are the ones that are most significant in the overall performance of the system. Towards the end of the chapter, we will draw a comparison between all the prototypes and discuss the outcome.

In order to understand the following results, we would like to describe some of the terms used for calculating the performance of the system. We broke the results down into two different main categories, True values and False values. Within these categories, there are two sub-categories for each. This concept of true and false values helps us categorize our detection logs into separate areas for further analysis and for gauging the performance of the system. We look at the meaning of each of these terms in order to see the difference and relevance of each of them:

- ***Objects***

An object is defined as the blob detected within a thermal frame, considered to be a person on the ground.

- **Subjects**
Subjects are the real persons (singular or multiple) on the ground who are being detected by the UAV system and are considered as objects within the frame once detected.

In the following formulae, n is any variable ≥ 0 i.e. n is non-negative.

- **True Positive (TP)**
True positive means that a detection has been made by the system and the number of objects detected in a frame is equal to the number of subjects present in the corresponding area on the ground.
 $Obj_n = Subj_n$; where $n > 0$
- **True Negative (TN)**
True negative means that no detection has been made and there are actually no subjects inside the frame at the moment the frame was captured on the thermal camera.
 $Obj_n = 0$; where $Subj_n = 0$
- **False Positive (FP)**
False positive implies that a detection has been made in such a way that the number of objects captured and recognized by the system is greater than the number of actual subject present on the ground. In other words,
 $Obj_n > Subj_n$; where $Subj_n \geq 0$
- **False Negative (FN)**
False negative is the type of detection where the system believes that there are no objects in the frame when in fact there are subjects on the ground within the frame area. Another condition for a false negative is that the system detects a number of objects that is lower than the actual number of subjects present in the frame on the ground.
 $Obj_n < Subj_n \parallel Obj_n = 0$; where $Subj_n > 0$

We break the rest of the chapter down into three main categories based on the prototype being discussed. Each section goes into the details of the test results for each of the prototypes.

5.1 Prototype A

Prototype A proved to be the basis of this research, even though the results were not very accurate. In Prototype A, as discussed in the previous chapter, we used the Lepton 50° camera with limited testing.

The first metric that we will discuss here is the surface type. For prototype A, we detected the subject on two different surfaces; grass and asphalt. The following chart gives us an overview of the results in terms of True and False values of detection on these two surface.

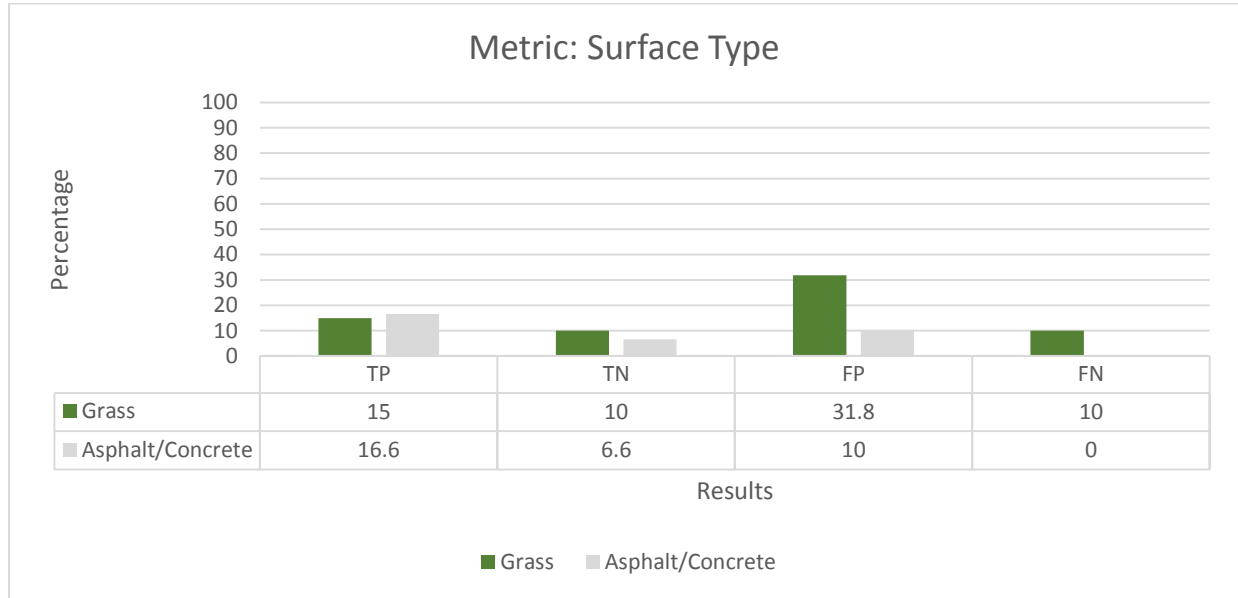


FIGURE 5. 1 PERFORMANCE OF PROTOTYPE A BASED ON SURFACE TYPE

In the above chart, we can see that for a test subject present on a grassy surface, the number of true positives is almost equal to the number of true positives for a subject standing on a concrete surface. The numbers for true negatives, where no subject was present and the system did not make any detection is also almost similar. A contrast can be seen for the results of false positives for both grass and asphalt. This is because of the differences in the ambient temperatures and the fact that with asphalt, the background stayed the same as well as the fact that there weren't any obstacles in the frame. On the other hand, for grass scenario, we can see detections for things other than humans that have a heat signature, for example trees. For false negatives, we can see that there's a huge difference between both the metrics as for grass we have false negatives, while there are no false negatives for a subject standing on an asphalt path.

For the second metric, we considered time of day. All the testing for this prototype was conducted at day time so the graph only shows a comparison between all the true and false values. On the Y axis of the following table, we can see the percentage of all the true and false values while the X axis lists them in the order TP, TN, FP and FN.

We can see that at day time, the Lepton 50° gives us results that are not very satisfactory and a whole system cannot be made dependent on such performance. In comparison to a total of 38.2% true detections, including both true positives and negatives, a high 61.8% of false positives

and negatives were recorded, meaning that the system does inaccurate detections and records false detection events at 1.6 times more than true or correct detections.

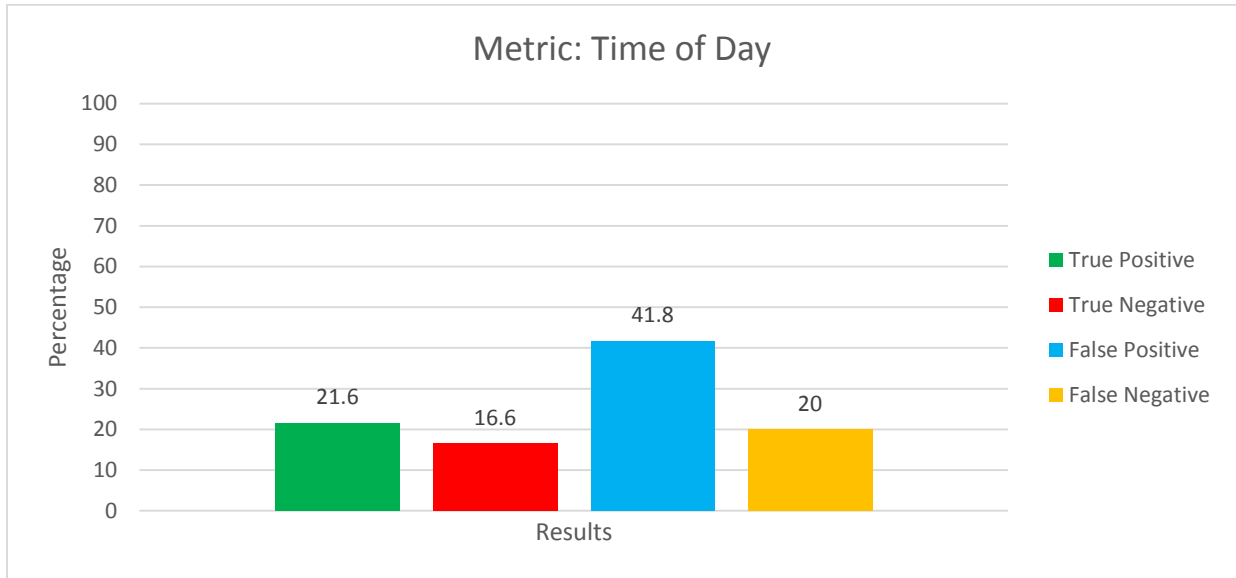


FIGURE 5.2 PERFORMANCE OF PROTOTYPE A BASED ON TESTS CONDUCTED AT DAY TIME

We look at the overall performance of the system by aggregating the results for all the metrics and giving an overview of the final result. This is done by adding all the true values to their corresponding true values and false values to their corresponding false value categories and then drawing a percentage of the totals. This gives us a fairly accurate view of the overall performance of the system based on all the metrics that were involved in the testing process.

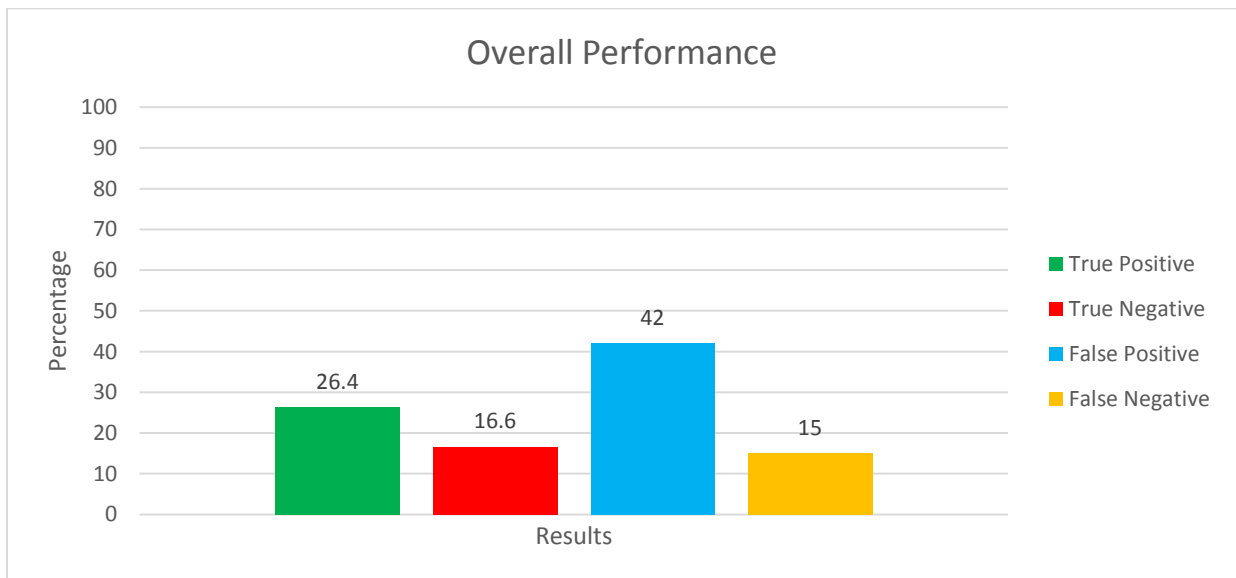


FIGURE 5.3 OVERALL PERFORMANCE OF PROTOTYPE A

We can see from the graph that when aggregated, the results give us a view of how good or bad the performance of this prototype is. Similar calculation methods are used for the rest of the prototypes. We can see that the number of false positives is 1.6 times those of true positives, meaning that prototype A makes 1.6 times more false detections (confusing other objects for the subjects) than it does true detections. The number of true and false negatives is same. To further simplify these results, we represent them in the following Pie chart.

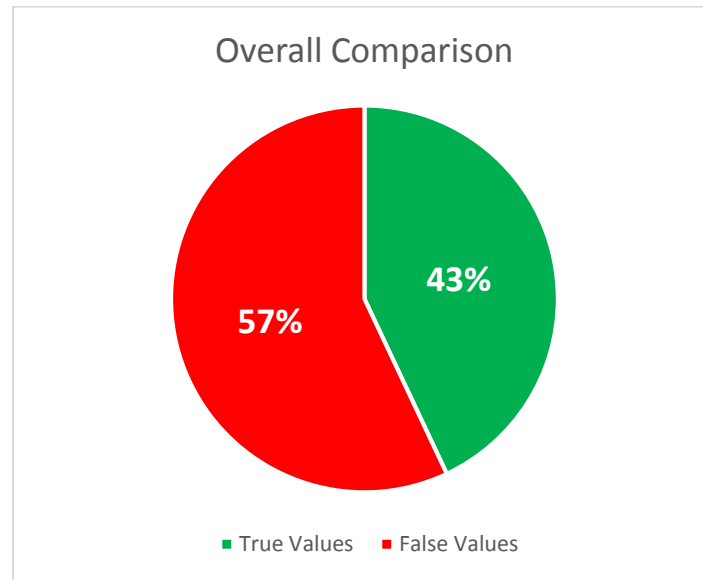


FIGURE 5. 4 PIE CHART SHOWING TRUE VS FALSE VALUES

From this chart, we can see that the system is not very efficient and that the number of false detections is higher than the true detections, with the former coming in at a total of 57% while the latter make up a total of 43% of the result set. This means that the system will make wrong decisions approximately 57% of the times.

5.2 Prototype B

For prototype B, many metrics were considered but for the results, we will only consider the most important and relevant ones. These results are also used to draw a comparison of prototype B with the other prototypes. As it turns out, the performance of prototype B was much better than that of prototype A. This is due to the fact that Lepton 25° gives us better results as well as the fact that proper test plans were generated and followed. Tests for prototype B were conducted both at day and night time.

We can see in the following graph that we tested for two different surface types at night time. We could not secure the use of a swimming pool at night time for experimentation therefore those values are not shown in the results. We can see that for night time, since ambient temperatures are lower compared to day time, the results are better defined and far more detections are made. The performance on grass surface at night is even better compared to asphalt or concrete because asphalt and concrete tend to store the heat from being in the sun all day while grass surfaces or soil tend to lose most of the heat due to shade and evaporation etc. No false negatives are assigned for night time grass testing because for all the frames that did have the subject in them a proper number of objects were detected and defined by the system.

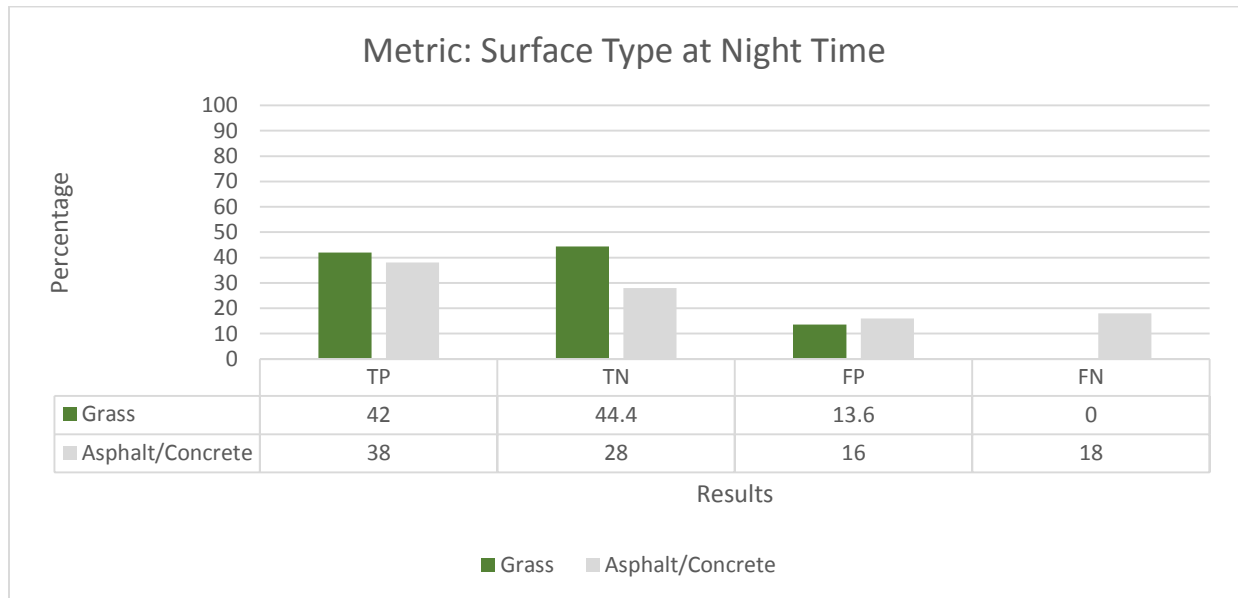


FIGURE 5.5 PERFORMANCE OF PROTOTYPE B BASED ON SURFACE TYPE AT NIGHT TIME

In the next graph however, we can see that we have conducted water tests for prototype B. These were conducted at day time and in two different ways. The first type of water tests included looking at subject who were swimming. There weren't many detections made because only the head or the arms are visible outside the water at a given time, reducing the surface area phenomenally. The second type of tests included asking subject B to partially submerge her body in the water, to mimic the movements of a person who is trying to survive a flood.

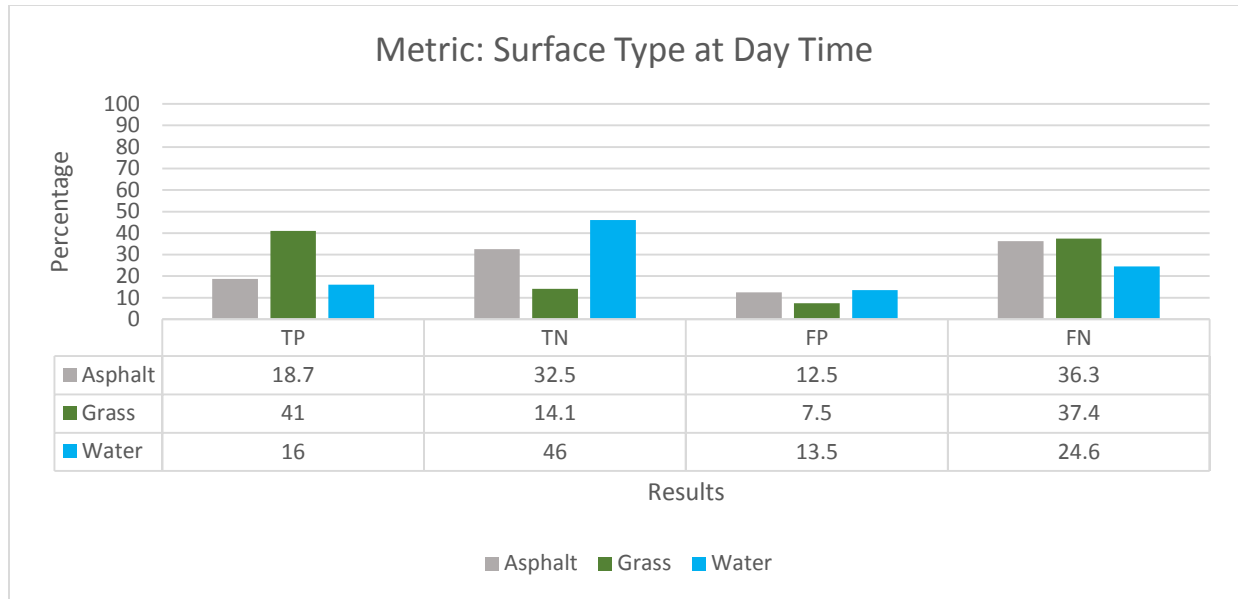


FIGURE 5.6 PERFORMANCE OF PROTOTYPE B BASED ON SURFACE TYPE AT DAY TIME

We can easily see that day time performance for Asphalt/Concrete and Grass are very different and not good compared to night time performance of the system. This is because of the different in ambient temperatures at day and night.

These differences are further simplified in the next graph where we can see a contrast being drawn between day and night time true and false values. We can visibly see that the performance of the system is much better at night time than at day time for the same kinds of tests.

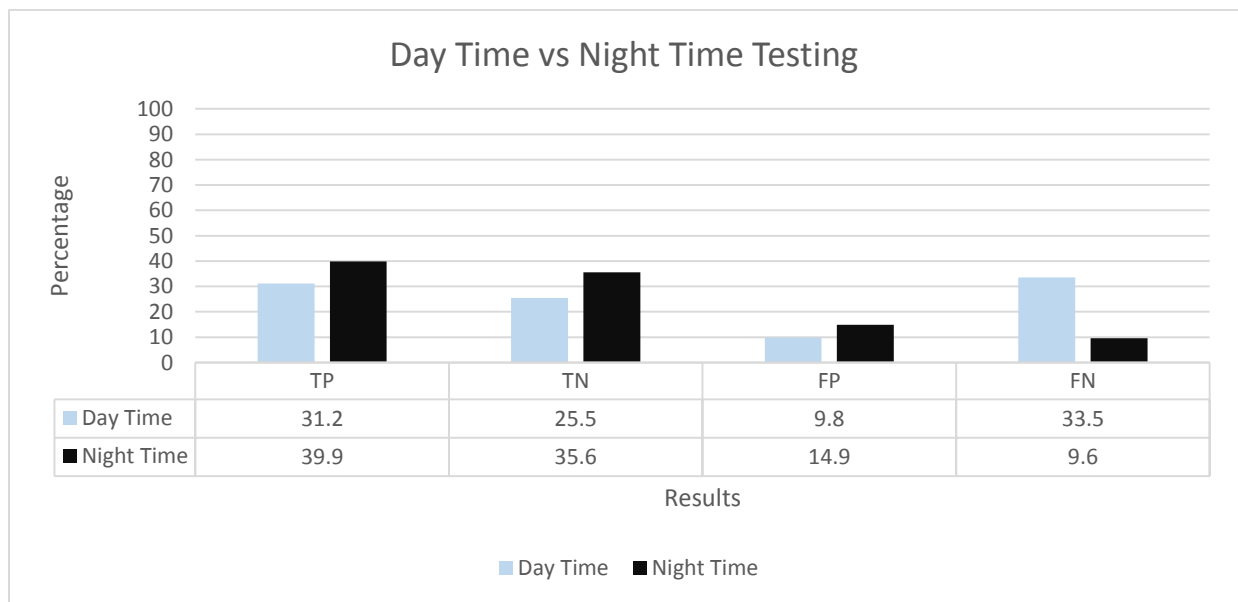


FIGURE 5.7 COMPARISON OF DAY AND NIGHT TESTING FOR PROTOTYPE B

This next graph aggregates the performance of the system over all the scenarios and gives us an overall view of how the system performed in terms of true and false values.

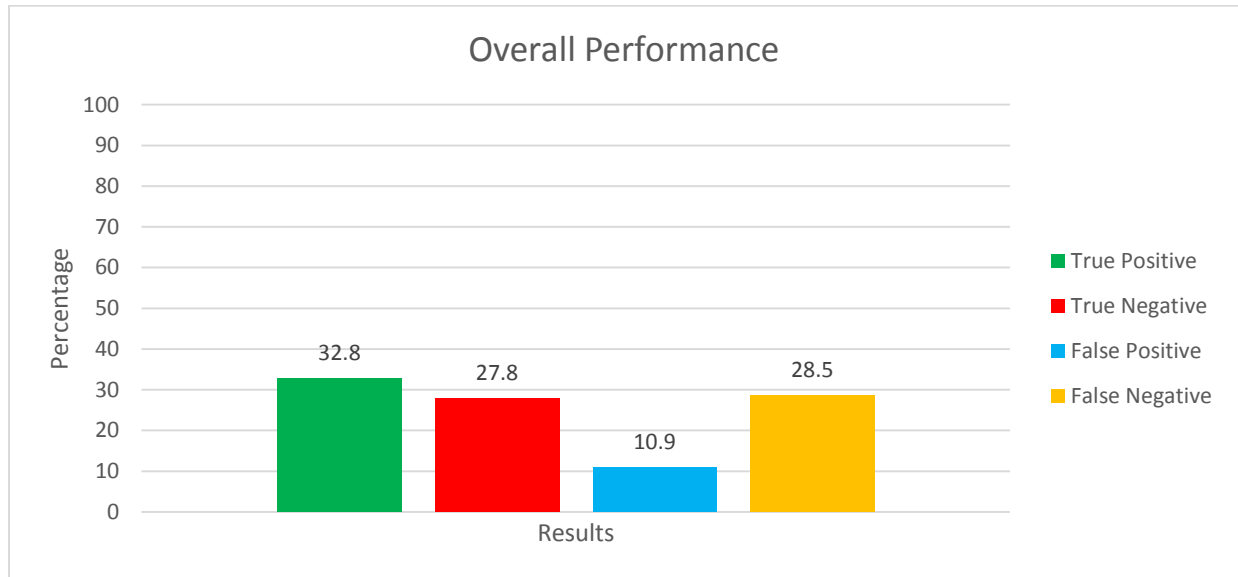


FIGURE 5. 8 OVERALL PERFORMANCE OF PROTOTYPE B

The reason for a high percentage of false negatives is because in the water tests, many times the system ignored the subjects when the subjects were in fact in the frame. Another reason is the asphalt tests where the temperature of the underlying asphalt path sometimes interfered with the heat signature of the subject and superimposed onto it, leaving the system baffled and thus ignoring the subject. We further simplify the overall performance results in the following pie chart. This pie chart represents all the true and false values for prototype B and gives us a simple comparison. Looking at the results, we can see that the system would give us a correct detection event approximately 61% of times while the error rate is about 39% of times. These numbers are much higher and better than those of prototype A but as we will see in sub-section 5.3, prototype C gives us much better results.

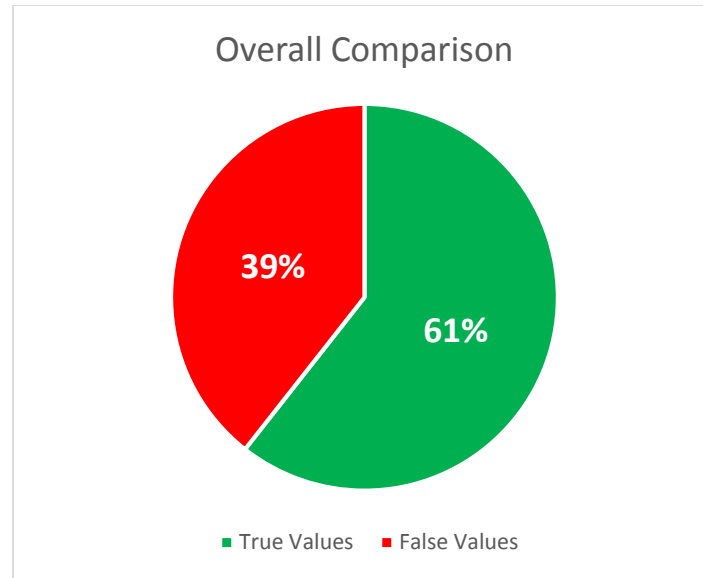


FIGURE 5. 9 TRUE VS FALSE VALUE COMPARISON FOR PROTOTYPE B

5.3 Prototype C

For prototype C, we considered a number of metrics while testing. Due to limited time and resources, all metrics could not be applied and the crashing of our UAV platform did a lot of damage to the experimentation process. Some of the metrics that we looked at included surface types, comprising of grass and asphalt. Earthquake scenarios were the only scenarios that were simulated for prototype C, following the high ratio of failure in prototype B for floods. Weather conditions were also taken into account, focusing on the subject standing in the shade as well as the sun on a grassy surface. All the tests were conducted at day time so only those results have been included in the time of day metric. We look at each of these individually, starting with the surface type metric.

In the following graph, we can see that the percentage of true positive values is higher for grassy surface compared to asphalt. True negatives, however, are lower for grass compared to asphalt are lower. This is because the tests were conducted in a location where the subject was not placed in isolation and the surroundings superimposed on the heat signature of the subject. False positives mostly occurred because of the lack of a shutter on the Lepton 25° used in these experiments, giving us a lack of flat field correction. However, grass surface experiments gave us a higher number of false negatives. This is due to the surroundings of the subject, with a house to the right of the frame and a long strip of shadow running along the house's length. This made the thermal sensor mistake the frame as having no subjects and did not detect any objects, especially in cases where the subject was standing in the boundary areas i.e. between the line separating the shadowy area and the sunny area.

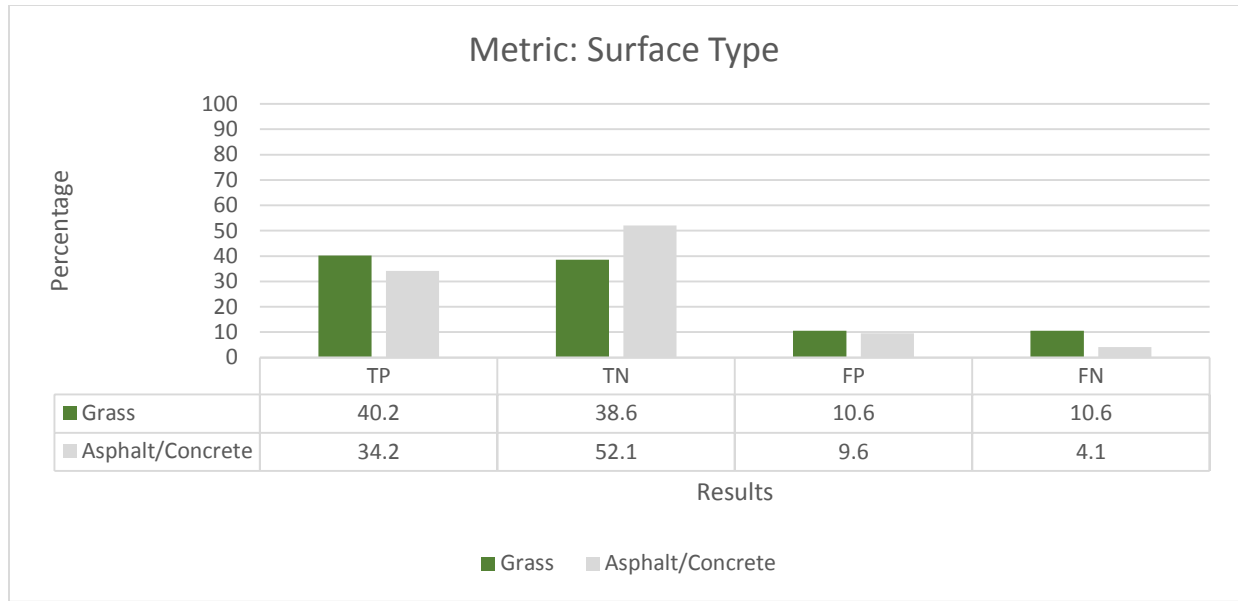


FIGURE 5.10 PERFORMANCE OF PROTOTYPE C BASED ON SURFACE TYPE

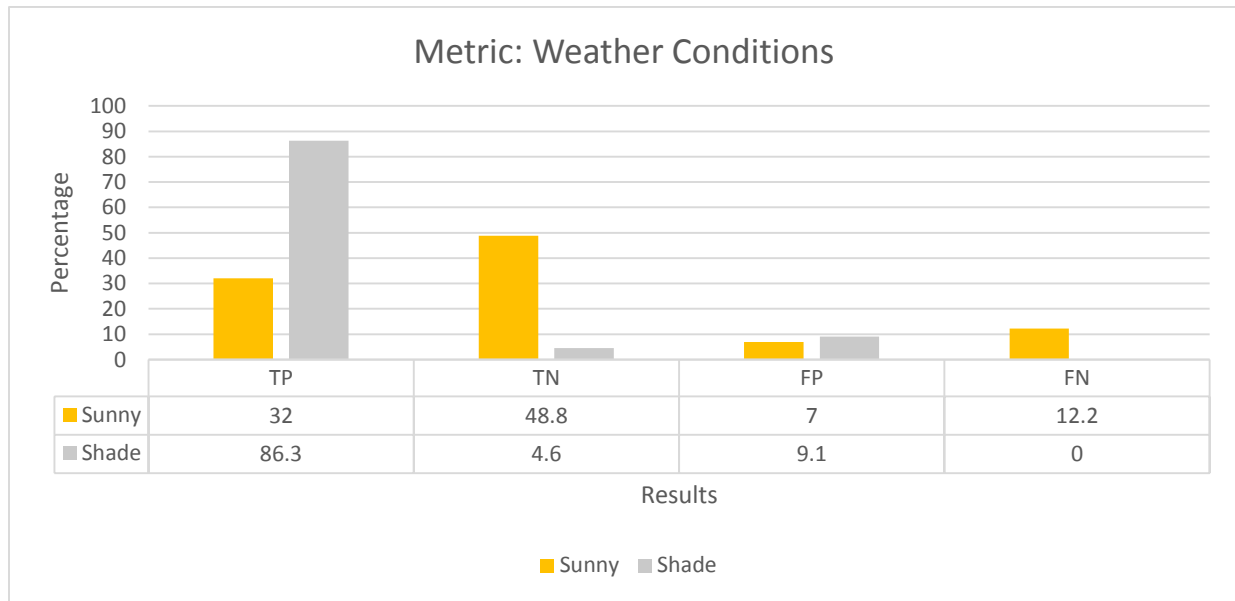


FIGURE 5.11 PERFORMANCE OF PROTOTYPE C BASED ON WEATHER CONDITIONS

In the next graph, we have shown a comparison between the detection results of a subject standing in the shade and in the sun. We can see that when in shade, the true positive values are increased phenomenally and are more than twice the number of true positive detections for when the same subject stood out in the sun. This is because the ambient temperature in the shade is much lower compared to the ambient temperature in the sunny part of a frame. This causes the heat signature of the subject to stand out in comparison to its surroundings, making it easy for the

subject to be detected. True negatives, however, are much higher for sunny locations compared to the shade. This mostly depends on the location we picked for testing. The values for false positives in both the metric considerations are fairly low and on the verge of being negligent when compared to the true values. False negatives show a crisp contrast between shade and sunny as no false negatives were declared for when the subject was absent from the shady frame while some false negatives were declared when the frame with a blank frame with the sun was captured.

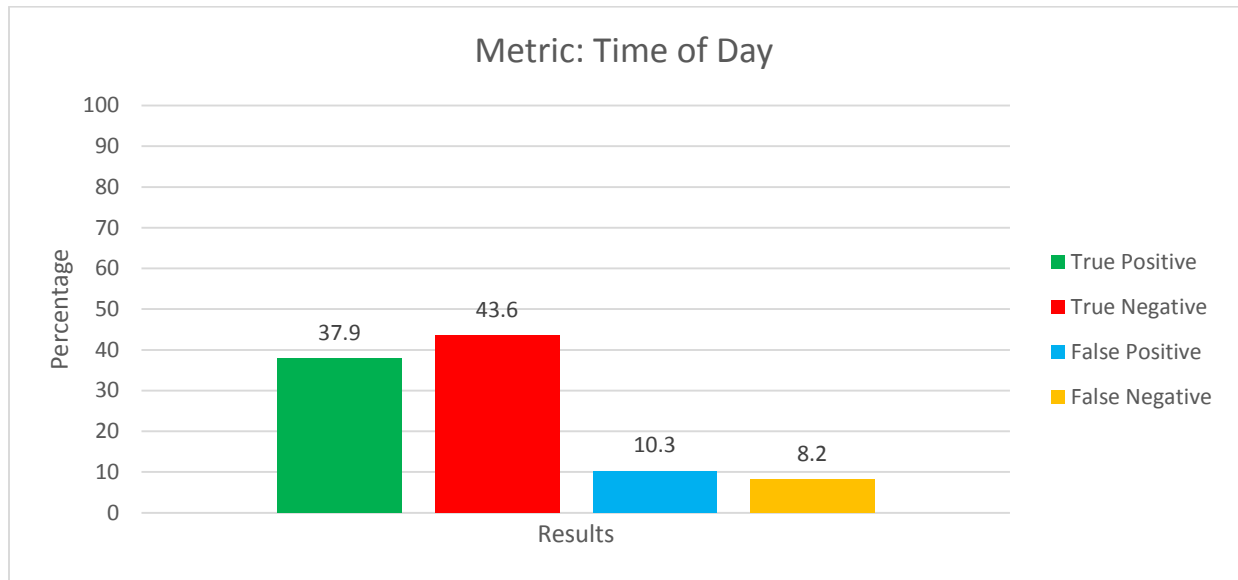


FIGURE 5.12 PERFORMANCE OF PROTOTYPE C BASED ON DAY TIME TESTING

For the time of day metric, we only considered day time values since that was the only time the tests were conducted. We can observe from the chart that true values are much higher compared to false values, making the system results much more reliable and in favor of correct detections.

For overall performance, we follow the previous technique of aggregating all the metric results and looking at the overview in a percentage setting where we can easily gauge the overall performance of the whole system. This overall view of the system takes into account all the metrics at once and gives us a true result that is easy to compare. The following pie chart further simplifies the overall result and helps us understand the contrast that has been drawn between the true and false values for the experiments conducted with prototype C. It was observed that the system made a correct detection decision based on the thermal image 82% of times compared to a small value of wrong detection events, recorded to about 18% of the total result domain.

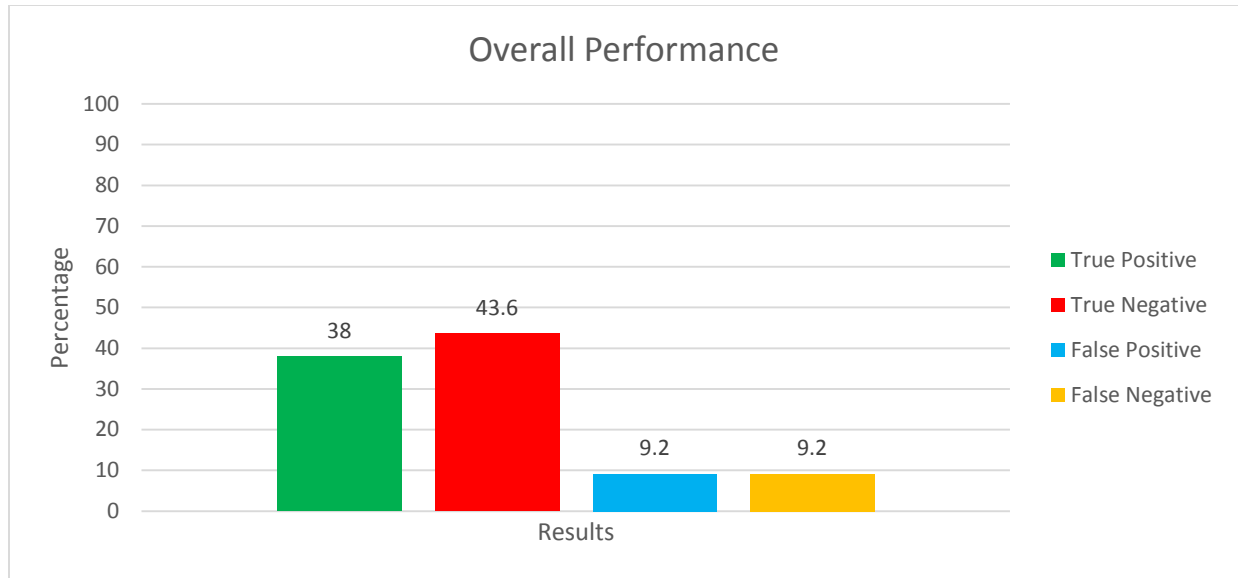


FIGURE 5. 13 OVERALL PERFORMANCE OF PROTOTYPE C

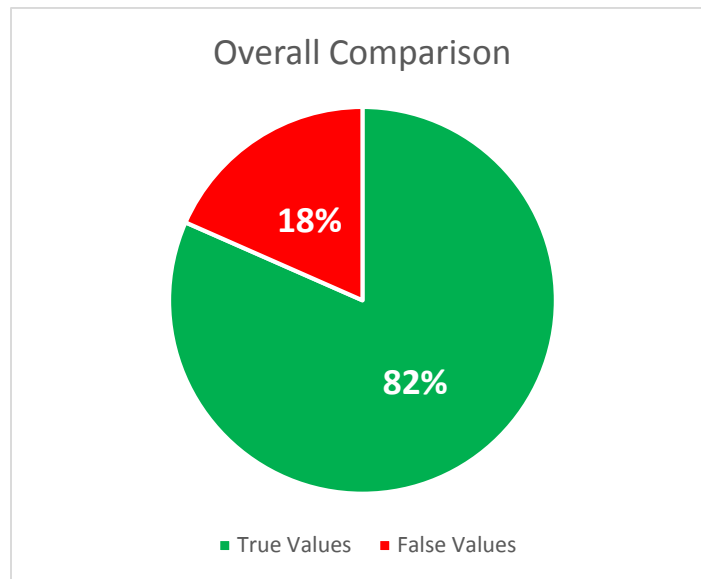


FIGURE 5. 14 COMPARISON OF TRUE AND FALSE VALUES FOR PROTOTYPE C

Based on these results, we can make the following deduce that the final prototype i.e. Prototype C, gave us the best performance in terms of person detection based on thermal images. The only downside of this prototype was the light weight UAV used. If a combination of the prototype B UAV and the prototype A software can be created, the system would further improve its accuracy. The use of both thermal and color camera improves the ease of sifting through the images once all the results have been logged. During the compilation of these results, we faced some problems when it came to older records of prototypes A and B because they did not have the

corresponding color images and they were also not logged properly. For prototype C, the use of color images made it easy for us to make the links between real images and thermal frames.

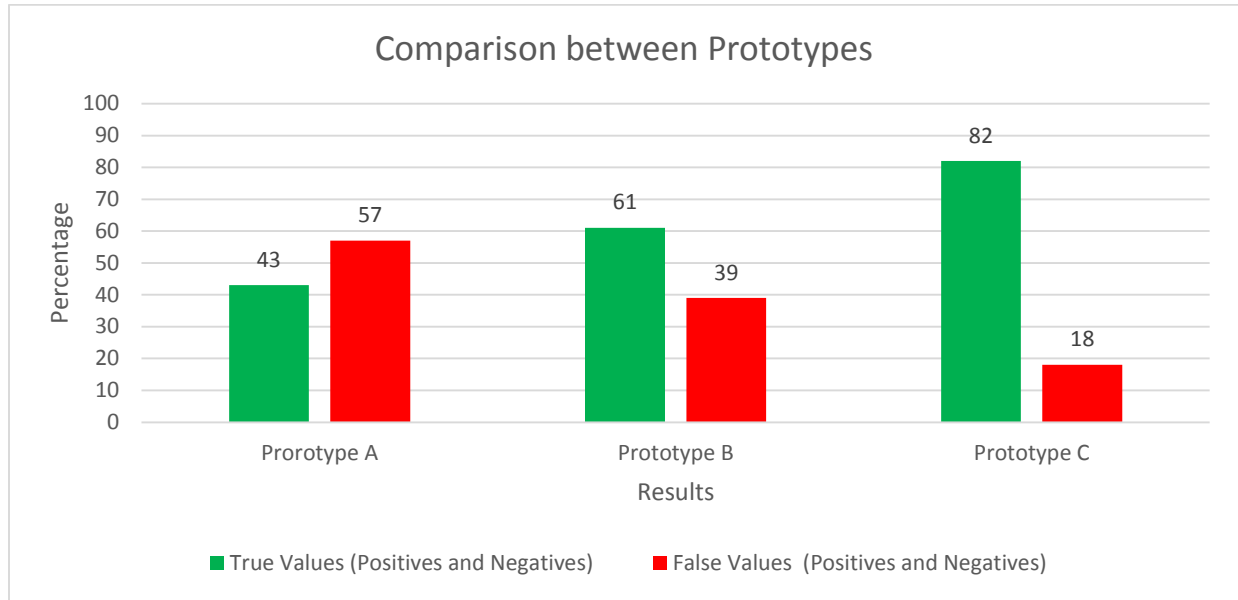


FIGURE 5. 15 COMPARISON OF OVERALL PERFORMANCE NUMBERS FOR ALL PROTOTYPES

It was also observed that the accuracy of the system is affected by many factors which have driven us to come up with an optimal deployment model which can help the system work in the most effective way, giving the best possible results. These optimal operational values based on the metrics in Chapter 4 as well as the results generated in this chapter are listed in the following table:

Metric	Scenario: Earthquakes
Time of Operation	Day Time
Altitude	20 meters
Weather Conditions	Dry (Sunny and Shade)
Surface	Grass and Asphalt/Concrete
Speed	2 kph
Weather	Dry

TABLE 5. 1 OPTIMAL OPERATIONAL RECOMMENDATIONS

The altitude metric was considered because as the altitude of the UAV changes, so does the surface area of the object inside the frame. This makes the system unstable as it is not yet mature enough to automatically calibrate its threshold values that are applied to the blob detection algorithm. At 20 meters, it was observed that the results are crisp and the true values increase. The system is not waterproof as of yet so it can only be used when it is dry outside, making it void for use in rain and snow. Speed of the UAV should be kept at 2kph or less, as higher speeds make the

camera either miss the subjects or blur them into the surroundings. This has partly to do with the placement of the cameras on the UAV body. This problem can be mitigated using a high quality three-axis gimbal, stabilizing the camera and making it immune to the UAV's movements. Finally, the system gives us the best results when used against the backdrop of a grassy or asphalt/concrete surface. The performance deteriorates when it comes to water detections, and therefore it is recommended for use in Earthquake scenarios, though it can be used for other scenarios as well, with lower accuracy.

Chapter 6

Conclusion

In this research we have presented a framework for a low cost UAV based person detection system. This system makes use of thermal imaging sensors as well as UAV flight data to detect people in a post-disaster terrain scan and then helps rescuers reach the survivors in a timely fashion so that a higher number of lives can be saved. The solution we present is innovative in that it provides an already available solution in a much more compact, and efficient package that is easy to operate, easy to scale and not heavy on the wallet. Person detection is done by applying algorithms onto thermal images captured from a thermal camera installed on a UAV, to be transmitted wirelessly to a base-station. We made this cost-effective by installing custom built components and modules that were improvised for use on UAVs for image capture and transmission, including writing custom software where necessary to get the results we wanted from the hardware sensors. We successfully made highly experimental hardware components work effectively in an integrated environment. We achieved near real-time person detection from the thermal sensor and Raspberry Pi.

Based on the preliminary results, a successful detection and recognition rate of up to 90% was observed at altitudes below 40 feet (12 meters) and air speeds of up to 15 kilometers per hour (~9 miles per hour). The results, therefore, can be categorized as promising and the system can be deemed ready for deployment in the field for real time rescue work. The system is capable of detecting humans in a variety of postures as subjects were detected in prone, crouching and standing positions. A number of test subjects were employed, including a 6 feet (~2 meters) tall male and a 5 feet (~1.5 meters) tall teenaged boy. We determined that we are able to conduct collaborative aerial surveys and assessment of disaster struck areas, using a swarm of UAVs.

Our system provides a robust solution for disaster rescue service and can be used for Search and Rescue (SAR) in the immediate aftermath of many common natural disasters like Earthquakes and Floods. The system can also be used in other disasters like Hurricanes, Typhoons, and Tsunamis etc. but only after the weather conditions have improved to within the operational limits of the system. Our system, if need be, can also be used for SAR in man-made disasters as well as non-disaster situations. This makes our system a truly versatile solution to all SAR activities.

6.1 System Limitations and Problems Encountered

This section of the Chapter talks about the problems encountered throughout the lifetime of the research. Any shortcoming in terms of performance of the system are also discussed here in detail.

Due to the lack of a physical protective case on most of the components used, our UAV system is susceptible to environment damage. This limits the operability of our system in some disaster situations for example, during heavy rains, the system cannot be deployed. The system can also be damaged in situations where high winds are a factor due to the size of the UAV.

Most of the primary hardware components used in this project were either highly experimental or not meant for this kind of usage. The FLIR Lepton camera was a recent release and came out as an iPhone extension module which we modified for use in our project. It was not designed to be used as a UAV mounted thermal imaging sensor, though some researchers had tested it with somewhat unsatisfactory results. Another example would be the Xbee radios which are not designed for data transmission and are generally used for telemetry purposes. We employed these antennae for transmitting data between the UAVs as well as the Ground Control Station. All of this experimentation with new equipment made initial integration and testing tough and faulty with minimal accuracy. These problems, along with others, are discussed in detail as follows.

The biggest issue we encountered, as mentioned above, was the Lepton camera. Since it is an iPhone hardware extension module, it was not designed for mounting on a drone for aerial thermal imagery. The sellers had made a custom break-out board for the camera, which was slightly loose, giving us unreliable probabilities of whether the camera will work in flight or not. Upon observing flight trends as well as the number of times the camera failed upon launch, we calculated a failure rate of almost 50% which is a lot. Another issue with the Prototype A of the camera was the resolution and image quality; it only gave us 60 x 80 pixels of data which could then be changed into images with thermal information. This highly limited our operational capabilities and stalled the process of deployment. This problem, however, was solved to some extent with the use of the Prototype B, which had the Lepton model with 2x zoom, giving better quality images, though the resolution still stayed the same. Prototype B, however, was also limited in that it had only a 25° field of view, making placement and maneuverability of the drone very hard. It also lacked the proper deployment of the Pi camera.

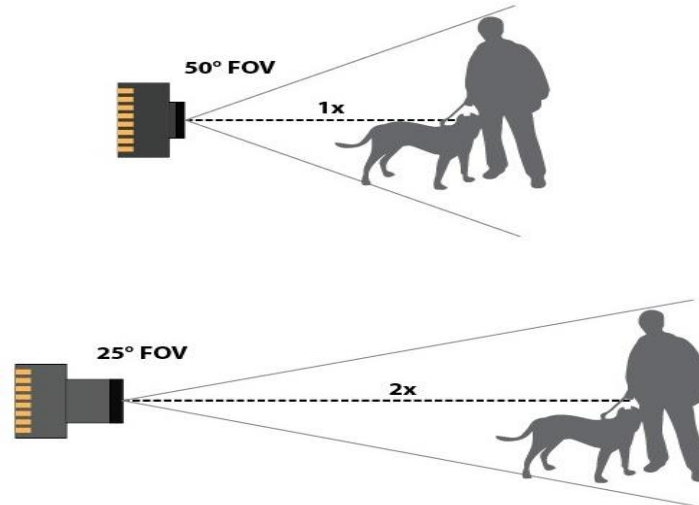


FIGURE 6.1 THE LEPTON'S TWO MODELS, WITH ZOOM AND FOV INFORMATION [11]

These problems were mitigated to some extent in the Prototype C which had an overall better deployment of modules on it. However, Prototype C lacked the inflight stability of the first two prototypes due to change of UAV.

Lack of hardware and engineering knowledge was proving to be a monumental issue since a lot of wiring and soldering was involved in the project. With the lack of real-estate on the drone, we had to make do with stretching and bending the wires that the camera was connected to, which, quite often, would either make the wires malfunction during operation or permanently damage them. This issue was resolved by soldering the wires to the breakout box in order to make it stable for long term use. Adding an increasing number of components to the UAV also had to be monitored closely since the stability of the craft depended on a weight balance.

The Raspberry Pi is a very powerful computer but it still lacks the ability to successfully run processing-heavy image processing and detection algorithms. This problem made us use a simple, less complex algorithm such as the MSER to tackle the issue of person detection in thermal images. If a more powerful machine can be made available that meets the cost effectiveness and size constraints of our research, more advanced algorithms can be used with background reduction and other techniques to make the person detection even more reliable.

Loss of the 3DR X8+ in an accident proved to be a mighty blow to the progress of the research since without a highly stable UAV, the whole system could have failed. The X8+, with its metallic body and stable weight, provided a platform that was reliable in harsh weather conditions and could withstand strong winds. The X8+ also provided us with a lot of surface area where we could add modules without severely affecting functionality of the craft. When we had to replace the X8+ with the CX-20, which was a much lighter and fragile model, we ran into a lot of problems. The biggest of these problems was the stability of the UAV since it was not meant to have so many modules attached to it. The addition of all the equipment also made the aircraft susceptible to winds and turbulence. Since the UAV itself was fairly light, it did not give us the

support that we needed in order for the platform to fly stably. This caused the UAV to crash a couple of times in windy weather. But in conditions where the winds was not very high, the UAV performed well and provided good results.

The Xbee radios used for the project came in two separate batches, and the first model was not compatible with the second one. This delayed our simulation of Prototype B as we couldn't have them connected to each other or the base station at the same time.

Another issue related to the Xbee was the MTU for data transmission. Xbee, at best, can send only 100 bytes of data. This is because Xbee radios were never meant to be used for data transmission but rather only for telemetry. The MTU available to us was not enough for the 120 kilobytes of data per message that we needed to transmit to the Ground Control Station. To counter this problem, we came up with the idea to packetize the data sent. This meant, making approximately 120 packets for every message. This in itself gave us a lot of trouble because data had to be packetized on board the Raspberry Pi, then those packets had to be sent back to the Ground Control Station. At the Ground Control Station, there are node-specific circular buffers that take the data from their specified node and waits for the terminating bit in the last buffer. Once that bit is detected, the buffer is full and the message has been received successfully. This message is then de-packetized and uncompressed at the Ground Control Station so that relevant data can be extracted from the message.

6.2 Future Work

The areas of person detection, peaceful drone technologies and disaster rescue and relief are a forever growing field of study, with advancements made every day. For our project, restrictions due to Federal Aviation Authority's rules about line-of-sight flights as well as security concerns of the Government and private citizens (due to the use of cameras), we had to cut short on some things which we plan to accomplish in the future. These are open problems that can be tackled and can be taken further by anyone taking up this project, developing it into a state-of-the-art disaster rescue and relief vehicle that can even be commercialized.

One of the major improvements that can be made is in the area of Person Detection Algorithms. With advancements in image recognition algorithms happening every day, we can improve the quality of detection in terms of accuracy. The Raspberry Pi is a powerful machine, but with future prototypes, we are sure that better, more advanced algorithms can be run on board the drone, making better detection possible remotely.

Thermal camera with better resolution and zoom properties, that are not very heavy or large, can be acquired in the future. Within a month of the purchase of the first Lepton prototype, the second one was available, which gave us much better results. This means that this area of technology is advancing fast and in the future, better cameras will be available for use on this project. An example of such a camera would be the FLIR TAU 160, which at the moment is expensive therefore did not make the cut.

Autopilot feature is another feature that can be added to this project and is planned for future development. With the use of GPS data that is already available to us on the drone, we can easily program and further develop our Ground Control Station so that the drone flies automatically on a given grid in a map, following waypoints and collecting data along the way. Even though this is discussed in detail in this research, it is yet to be implemented in real life experiments. This can prove very useful as the drones already have such capabilities, given the use of the Pixhawk. This automation of the flight would help in future, real life deployment of the system, where the drone would automatically carry out missions, probably on a daily basis. This, along with the deployment of multiple drones in a swarm, can help with large area coverage and better detection results through co-ordination. Multiple drones can cover large areas, with multiple functionalities and capabilities. Drones can co-ordinate and assist each other too.

Real time view capabilities can also be introduced for manned missions so that a better understanding of the overall terrain can be made possible. These days there are numerous real time view systems that can be integrated with the Raspberry Pi camera module onboard the UAV. This can provide us with both real time view of the flight as well as the recorded images we need for later manual terrain recognitions. Systems like the 3D Robotics LiveView™ can also be integrated with the current system for real time flight monitoring capabilities for manual flights.

We can also work on waterproofing the system so that it can be a truly versatile system in terms of its operability. Once waterproofed, it can be deployed in scenarios that have rain and can be used in locations with very high humidity or even close to water surfaces without the operators being worried about the safety of the UAV or the onboard modules.

The last thing we would like to talk about is the use of better radios. The Xbee radios that were used in this project, according to our land tests, only gave a range of approximately 300 meters with Line of Sight visibility. This can be improved but with the use of unidirectional antennae, which would deteriorate the data transmission capabilities of our project. Better radios, with greater MTUs and range would give our project the capability to go further and cover more ground, without signal degradation or data loss. This would also bring the computational cost down to a minimum, since additional computational complexities like data fragmentation and defragmentation as well as buffering would not be involved.

Appendix

Sample output of Flight Log

The following snapshot shows a sample of the flight log saved after each flight in .csv format. The log keeps the following information in relation to each incoming packet of data:

Timestamp (Date and Time), Longitudes and Latitudes (GPS Co-ordinates), Altitude (Meters), Compass heading (Degrees), Airspeed (kph), Groundspeed (kph), Thermal and Color images (png format), and the signal strength information of the radios (RSSI).

1	Timestamp	Longitude	Latitude	Altitude	Heading	AirSpeed	GroundSpeed	ThermalImage	CameraImage	RSSI
2										
3	10/25/2015 12:26	-76.8082967	39.2300436	0.06	161	0.09	0.09	1445790410.png	1445790410.png	40
4										
5	10/25/2015 12:26	-76.8083152	39.2300229	6.18	160	0.22	0.22	1445790413.png	1445790413.png	40
6										
7	10/25/2015 12:26	-76.8083067	39.230023	7.72	160	0.17	0.17	1445790416.png	1445790416.png	40
8										
9	10/25/2015 12:26	-76.8083092	39.2300238	8.34	159	0.29	0.29	1445790419.png	1445790419.png	40
10										
11	10/25/2015 12:27	-76.8083113	39.230019	8.96	159	0.12	0.12	1445790422.png	1445790422.png	40
12										
13	10/25/2015 12:27	-76.8083101	39.2300201	9.7	161	0.51	0.51	1445790425.png	1445790425.png	40
14										
15	10/25/2015 12:27	-76.8083069	39.2300202	10.48	160	0.07	0.07	1445790428.png	1445790428.png	40
16										
17	10/25/2015 12:27	-76.8083071	39.2300204	10.2	162	0.08	0.08	1445790431.png	1445790431.png	40
18										
19	10/25/2015 12:27	-76.8083079	39.2300232	9.43	160	0.03	0.03	1445790434.png	1445790434.png	40
20										

References

- [1] Murphy, R. "Fixed- and Rotary-Wing UAVs at Hurricane Katrina," 2006 IEEE International Conference on Robotics and Automation, May 15-19, 2006.
- [2] Murphy, R. (2015, May) Robin Murphy: These robots come to the rescue after a disaster [Video file]. Retrieved from http://www.ted.com/talks/robin_murphy_these_robots_come_to_the_rescue_after_a_disaster.html
- [3] J. Portmann, S. Lynen, M. Chli, and R. Siegwart, "People detection and tracking from aerial thermal views," in Proc. IEEE Conf. on Robotics and Automation, 2014.
- [4] P. Molina, I. Colomina, T. Victoria, J. Skaloud, W. Kornus, R. Prades and C. Aguilera (2012) Searching lost people with UAVS: The system and results of the CLOSE-SEARCH project. XXII Congress of the International Society for Photogrammetry and Remote Sensing, Melbourne, Australia, August 25 - September 1, 2012
- [5] Rosendall, P. (2008). "Person detection: Unmanned system and small sensor applications." Thesis (S.M.)--Massachusetts Institute of Technology, Dept. of Aeronautics and Astronautics, 2008. Includes bibliographical references (p. 97-99). Retrieved from <http://hdl.handle.net/1721.1/47796>
- [6] X8+. 3D Robotics Inc. Retrieved from <http://3drobotics.com/x8/>
- [7] Model Aircraft Operations (2015, March). Federal Aviation Administration. Retrieved from https://www.faa.gov/uas/model_aircraft/
- [8] Pri, A. (2015, July 31). Cheerson CX-20 Auto-Pathfinder Quadcopter Review and Flight Experience. Retrieved from <http://www.quadcopterflyers.com/2015/07/cheerson-cx-20-auto-pathfinder-quadcopter-review.html>
- [9] Raspberry Pi 2 Model B. Raspberry Pi Foundation. Retrieved from <https://www.raspberrypi.org/products/raspberry-pi-2-model-b/>
- [10] 3DR Pixhawk. 3D Robotics Inc. Retrieved from <https://store.3drobotics.com/products/3dr-pixhawk>
- [11] Flir Lepton. Flir Systems Inc. Retrieved from <http://www.flir.com/cores/content/?id=66257>

- [12] Camera Module. Raspberry Pi Foundation. Retrieved from <https://www.raspberrypi.org/products/camera-module/>
- [13] XBee-PRO® 900HP Datasheet – Digi International Inc. Retrieved from http://www.digi.com/pdf/ds_xbeepro900hp.pdf
- [14] 3DR uBlox GPS with Compass Kit. 3D Robotics Inc. Retrieved from <http://store.3drobotics.com/products/3dr-gps-ublox-with-compass>
- [15] Teutsch, M.; Mueller, T.; Huber, M.; Beyerer, J., "Low Resolution Person Detection with a Moving Thermal Infrared Camera by Hot Spot Classification," Computer Vision and Pattern Recognition Workshops (CVPRW), IEEE Conference on, pp.209-216, 23-28 June 2014.
- [16] DroneKit by 3D Robotics. Retrieved from <http://dronekit.io/>
- [17] MAVProxy. Retrieved from <http://tridge.github.io/MAVProxy/>
- [18] J. Matas, O. Chum, M. Urban, and T. Pajdla. "Robust wide baseline stereo from maximally stable extremal regions." Proc. of British Machine Vision Conference, pages 384-396, 2002.
- [19] Y. Tsunemi, T. Ishii, and M. Murata. "Imaging Solutions for Search & Rescue Operations." NEC Technical Journal, Vol.9 No.1, January, 2015.

